DYNAMICS OF DENSE POLYMER SYSTEMS: COMPUTER SIMULATIONS AND ANALYTIC THEORIES

JEFFREY SKOLNICK

Molecular Biology Department, Research Institute of Scripps Clinic, La Jolla, California

and

ANDRZEJ KOLINSKI

Department of Chemistry, University of Warsaw, Warsaw, Poland

CONTENTS

Advances in Chemical Physics, Volume LXXVIII, Edited by I. Prigogine and Stuart A. Rice.
ISBN 0-471-52666-5

I. INTRODUCTION

The elucidation of the mechanism by which an individual polymer chain moves in a concentrated solution or in a polymer melt (a viscoelastic liquid in which all the constituent molecules are polymers) has been among the central problems in polymer physics for over 40 years.[1,2] In addition to the complications arising from the effects of internal excluded volume on chain dynamics, there is the additional complexity in a melt due to the noncrossing constraint between the individual polymer chains. The problem of polymer melt dynamics is of interest not only in its own right as an example of an extremely complicated many-body problem, but also because its solution would have practical applications to the areas of polymer flow rheology, polymer adhesion, and polymer failure.[1] Thus considerable effort has been expended over the years to develop an effective single-particle picture capable of describing the dynamics of the chains in the melt. In this chapter we shall review a number of theoretical approaches to the solution of this problem.[3–22] Because of its inherent complexity, computer simulation techniques[20–24] and analytic theory[3–22] have been applied to explore the dynamics of entangled polymer systems.

A. Experimental Phenemonology

Before presenting an overview of the various theories that have been applied to treat melt dynamics, it is appropriate to summarize the salient experimental phemonenology that any successful theory must ultimately rationalize and encompass. Among the important characteristics of any given polymer property is the dependence of the property on molecular weight M (equivalently

the degree of polymerization, n). In many cases, the absolute magnitude of a given property has proven extremely difficult to calculate, and the elucidation of the scaling of this property with M has been a major focus of various theories.

For a polymer melt composed of linear chains, the center of mass diffusion coefficient scales with n as[1,25-32]

$$D \sim n^{-1} \text{ when } n < n_{c'}, \tag{1a}$$

and with a further increase in n,

$$D \sim n^{-2} \text{ when } n > n_{c'}, \tag{1b}$$

where $n_{c'}$ is a crossover value of the degree of polymerization. However, more recent experiments have called into question whether the scaling embodied in Eq. (1b) is the asymptotic behavior.[33] Substantially stronger scaling with molecular weight has been reported[33], and in the case of concentrated polymer solutions Phillies[34] has found that a stretched exponential of the form

$$D = D_0 \exp(-\alpha c^{\nu}) \tag{1c}$$

fits experimental data extremely well. Here D_0 is the diffusion constant of the polymer at infinite dilution which scales as M^{-b} with b in the range 0.5–0.55, $\alpha \sim M$, and ν is molecular weight dependent crossing over from $\nu = 1.0$ to $\nu = 1/2$ as M increases.[11,12] Thus the question of the molecular weight dependence of D is not resolved.

Another transport property that has been extensively studied is the zero frequency shear viscosity η, which depends on n as follows:[3,26]

$$\eta \sim n^{1} \text{ when } n < n_e \tag{2a}$$

and

$$\eta \sim n^{3.4} \text{ when } n > n_e. \tag{2b}$$

Observe that the value of the crossover degree of polymerization for viscosity and diffusion are unequal. Typical experimental data give n_e' of about $5n_e$.[35] Why the crossover values are different for the viscosity and the self-diffusion coefficient is not understood.

For a number of theoretical reasons[1,35] it has been questioned whether Eq. (2b) is the limiting power law behavior of η. A range of exponents of η has been reported, but the values tend to lie in the range 3.3–3.7, with 3.4 being

the most prevalent.[3,35] A major conceptual difficulty with the 3.4 power law dependence arises from the following: In a polymer melt, the static excluded volume effect giving rise to chain expansion is screened and the mean square radius of gyration $\langle S^2 \rangle$ scales as $n^{1.0}$.[1,36] As pointed out by Colby et al.[35] the time required for molecules to diffuse a distance on the order of the radius of gyration is

$$t_d = \langle S^2 \rangle / D. \tag{3a}$$

Thus $t_d \sim n^{3.0}$ if Eq. (1b) holds.

On the other hand, the time scale for stress relaxation,

$$\tau_0 = J_e^0 \eta \tag{3b}$$

where J_e^0 is the recoverable shear compliance (a molecular weight independent quantity in the limit of large M[1,26]). Hence, taking Eqs. (2b) and (3b) together implies that $\tau_0 \sim n^{3.4}$. In other words, if $\tau_0 \sim n^{3.4}$, then chains will move many radii of gyration before they undergo orientational relaxation. This apparently "nonphysical" result, when juxtaposed with the predictions of the reptation model of polymer melt dynamics, has led to the belief that in the asymptotic limit η should scale as $n^{3.0}$. Thus far, only one experiment by Colby et al.[35] on polybutadiene claims to find this n^3 behavior. However, these series of measurements, while clearly an experimental tour de force, have not been universally accepted as providing convincing evidence for the $n^{3.0}$ power law behavior of n.

Whatever the final resolution of this controversy, it is clear that as the length of the chains in a polymer melt increases, the behavior of the system changes drastically. The problem remains to identify the cause of this change in behavior; a reasonable qualitative explanation is that as the size of the chains increase, chain entanglements of some kind become important.

Thus far we have discussed the behavior of a melt of linear chains, which are by far the most extensively studied. However, rings are of intense interest because of the reptation model of polymer melt dynamics which asserts that for distances on the order of $\langle S^2 \rangle^{1/2}$, the other chains act to confine the chain of interest to a tube.[4-8,37] Thus, the dominant motion of the chain of interest involves the slithering down the tube, defined at zero time. In the reptation model, the motion of the ends is extremely important. Rings being entirely devoid of chain ends should, therefore, move substantially slower.[38] Experimentally, this doesn't appear to be the case. Melts of polymer rings have a lower viscosity and appear to be less entangled than the corresponding linear chains.[39,40] Roovers[40] has reported a scaling of η with n that is consistent with Eq. (2b); however, the absolute magnitude of η is less. Admittedly, due

to synthetic difficulties, the range of molecular weights measured is substantially smaller than for linear chain melts; nevertheless, the rings that have been studied do crossover into what is considered the entangled regime; i.e., the regime where the polymeric nature of the medium is influencing the behavior of the chains.

B. Entanglements: An Overview

What is immediately apparent from the overview given above of the experimental phemonenology is that as the length of the chains comprising the melt increases, the chains behave differently; the origin of these effects has been ascribed to entanglements of some sort between the various chains.

What is the nature of these entanglements? One picture that comes to mind is that the chains form knots. Thus, one chain is trapped by a knot formed by another chain until one of the two ends comes through, and therefore, disengages the entanglement.[6,18] If this is true, the question arises as to how mobile the entanglements are. One might envision that these slip knots are basically immobile, for times, on the order of the τ_0, and if so the knots could therefore form the tube conjectured by reptation theory. Another possibility is that, in fact, the knots are not rigidly held in space but are quite mobile.[18] Thus the chains are not confined to a tube. Rather, the internal configurational relaxation can occur relatively rapidly, but the disengagement of the chain from the knots is the rate-determining step.

There is an alternative view of entanglements.[9,14,16] This viewpoint, while conceding that the disengagement of knots will contribute to the relaxation, holds that this isn't necessarily the dominant process. Rather, a chain need not be confined by knots to be dynamically entangled—looping of one chain around the other can work just as well. That this effect can be important is motivated by the analogy with tangled fishing line. Topologically, in tangled fishing line, there are no knots whatsoever, yet one loop gets trapped by another loop until there is a tangled mess. Thus entanglements are viewed to be intrinsically dynamic in nature, with the surrounding chain environment at intermediate times (corresponding to distances on the order of $\langle S^2 \rangle^{1/2}$) being viewed as quite fluid, much like in a small molecule liquid.

Unfortunately, experiment does not get at the exact nature of the entanglements. Based on estimates of the crossover behavior of the viscosity, whatever they are, entanglements are rare, occurring on the order of a hundred monomer units or so.[3] Computer simulations are an especially powerful technique for elucidating, at least in a qualitative sense, the microscopic mechanism of various physical processes;[20] the nature of the motion in a polymer melt in not an exception. However, the simulation of polymer melt dynamics is not a trivial matter. One must simulate a sufficiently large number of long chains for long times in order that entangled behavior be exhibited.[23] As discussed

in further detail below, this is a nontrivial task. Here we point out that the simulations scale at least as the fourth power of n.

C. Rouse Model

One of the most surprising consequences of the experimental observations embodied in Eqs. (1) and (2) is that low molecular weight melts behave like Rouse chains, which is the simplest model for the dynamics of a polymer chain at infinite dilution.[41] In this model hydrodynamic interactions (the perturbation of the solvent flow surrounding one monomer due to the presence of the other monomers) are ignored, as are excluded volume effects.[41,42]

In what follows, the behavior of a Rouse chain will be required; we summarize here the salient features of the model. Qualitatively, the motion of a chain composed of identical monomers is isotropic at all times. For a chain composed of n monomers, the self-diffusion coefficient constant D_{Rouse} scales like n^{-1}. Furthermore, the mean-square displacement of the center of mass, $g_{\text{cm}}(t)$, is related to the self-diffusion coefficient, at all times t, by

$$g_{\text{cm}}(t) = 6Dt. \tag{4}$$

In the limit of very long chain lengths, the average mean square displacement of a bead exhibits the following behavior as a function of time:

$$g(t) \sim t^{1/2} \qquad t < \tau_{\text{Rouse}}, \tag{5a}$$

where τ_{Rouse} is the longest internal relaxation time and describes the decay of the end-to-end vector. τ_{Rouse} scales like $n^{2.0}$ if excluded volume effects are neglected. For distances such that $g(t)$ is appreciably greater than $2\langle S^2\rangle$,

$$g(t) = 2\langle S^2\rangle + 6Dt. \tag{5b}$$

Finally, the zero frequency shear viscosity scales like τ_{Rouse}/n, and thus the scaling behavior of Eq. (2a) is recovered.

D. Reptation Model

While the Rouse model has proven to be remarkably successful at characterizing the low molecular weight behavior of polymer melts, it cannot account for the enhanced dependence on molecular weight of D and n as the length of the chains increase.[25-34] The first class of models that proved capable of almost reproducing the molecular weight dependence of *both* the diffusion constant and the zero frequency shear viscosity is the reptation model.[4-8] It was originally proposed by de Gennes[4] to describe dynamics of a polymer chain moving in a gel, and later was fully developed by Doi and Edwards to apply to a polymer melt.[5-8] Since this is a widely accepted model against

which all alternative theories have had to compete, it is appropriate here to summarize its features. We focus here on its application to linear chains.

In the original reptation model,[1,4-8,37] one imagines that the surrounding chains produce entanglements that remain *static* for times on the order of the longest internal relaxation time. The beauty of this approach is that an extremely complicated many-body picture is reduced to a very simple single particle picture, namely, the dynamics of an isolated chain confined to a tortuous (Gaussian) tube. Lateral motions of the chain are always extremely limited, and the only way the chain can move distances on the order of the radius of gyration is by slithering out the ends of the tube, in a snake-like motion. The assertion that the dominant long wavelength motion is longitudinal, and essentially down the chain contour defined at zero time, is the fundamental assumption of the reptation theory and all its variants.[1,4-8,37,43-45] A schematic picture of the chain motion is presented in Fig. 1.

The scaling with chain length of the various properties can be readily derived.[46] Internally, the chain behaves like a Rouse chain; the only problem is that it must now travel a mean square distance on the order of the contour length, $L \sim n$, in order to relax its conformation. Thus the terminal or longest relaxation time τ_R is obtained from

$$\tau_R \sim L^2/D_{\text{Rouse}} \sim n^3. \tag{6a}$$

However, with respect to the laboratory fixed frame, the molecule has moved appreciably less, on the order of $\langle S^2 \rangle$, if one assumes that the tube obeys Gaussian statistics. Hence the diffusion constant with respect to the laboratory fixed frame is obtained from

$$D \sim \langle S^2 \rangle / \tau_R \sim n^{-2}. \tag{6b}$$

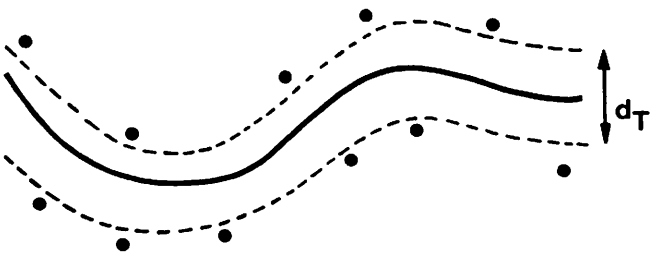

Figure 1. Schematic representation of chain motion in the reptation model. Owing to entanglements with other chains (solid circles), the chain of interest is confined to a tube for times on the order of the longest internal relaxation time; d_T is the diameter of the tube.

Observe that the long chain limit of the self-diffusion coefficient, Eq. (1b), is recovered.

To obtain the dependence on n of the shear viscosity, Doi and Edwards,[6-8] make the further assumption that there is a rubber-like (elastic) response of the melt at short times. Basically, in the short time limit before the chains have a chance to flow, it is impossible to differentiate the behavior of a melt where the entanglements provide the restraining influence, from a rubber where all the chains are covalently cross linked. Unlike the rubber case, the entanglements in a melt are not infinitely long lived, and thus the behavior of a melt is distinct from that of a rubber at longer times. Coupling the assumption of a short time rubbery response with longer time motion down the tube gives

$$\eta \sim \tau_R \sim n^3. \tag{7}$$

Observe that this is not quite the 3.4 power of n, found experimentally for the zero frequency shear viscosity[3,26] (see Eq. 2b); nevertheless, it is close. This has given rise to the conjecture that the $n^{3.4}$ power dependence of η is not the asymptotic behavior, rather it is indicative of a crossover regime.[35,37]

Subsequent work by Graessley provided a means of estimating the magnitude of D and η from reptation theory.[37] The reptation model, typically, overestimates η by about an order of magnitude, but overall it does a rather good job of estimating D.[1,35,37]

Let us compare the behavior of the single-bead autocorrelation function $g(t)$, obtained from a reptation model with the Rouse model.[4,5,46] For distances less than the tube diameter d_T, the chain is unaware that there is a constraining environment, and consequently simple Rouse behavior is recovered. Namely,

$$g(t) \sim t^{1/2} \qquad \text{if } g(t) < d_T^2. \tag{8a}$$

As time further increases, the chain now experiences the restraining effects of the tube and undergoes internal Rouse dynamics in a randomly distributed tube. Hence for times up to τ_{Rouse},

$$g(t) \sim t^{1/4}. \tag{8b}$$

The chain then undergoes free diffusion down the tube, thereby giving

$$g(t) \sim t^{1/2} \qquad \tau_{\text{Rouse}} < t < \tau_R. \tag{8c}$$

Finally, in the free diffusion limit,

$$g(t) \sim t. \tag{8d}$$

Similar considerations indicate that there should be a range of times for which the mean square displacement of the center of mass scales, like $t^{1/2}$ for times less than τ_R but greater than τ_{Rouse}.[20]

While the basic physical picture is quite reasonable for a regular gel, for which the reptation model was originally derived; it is not at all clear the same picture obtains when everything moves on the same time scale. The reality of a spatially fixed tube has been questioned by Fujita and Einaga,[9,10] by Kolinski, Skolnick, and Yaris,[16,17,23,47-49] and Fixman[18,19] for melts and concentrated solutions of linear chains, by Fixman[15] for concentrated solutions of rod-like polymers, and by Baumgartner and Muthukumar[50,51] for chains in a random static medium.

Thus, in the past several years the validity of the original reptation model has been examined.[9-12,15-19,34,47-51] There are two points that need to be clarified. First, is the fundamental assumption that stress relaxation arises from reptation-like motion correct? If so, is there a well-defined tube for motions on the scale of the radius of gyration?.

The examination of what is known about the nature of the dynamics in dense polymer systems is the focus of this chapter, the outline of the remainder of which is as follows. In Section II we present an overview of computer simulation results on multichain dynamics. In Section III we summarize the results of recent analytic theories of polymer dynamics and point out the agreements and disagreements with the simulation results. Section IV concludes the chapter with an overview of the status of the field.

II. COMPUTER SIMULATIONS

A. Dynamic Monte Carlo Results

The problem immediately encountered in an attempt to simulate the long-time dynamics of a dense polymer system is that one must have the ability to study sufficiently long chains for sufficiently long times so that one can verify that the scaling behavior of D and τ_R are reproduced by the simulation. One possible way of simulating systems into the crossover regime is to employ a lattice representation of the polymer melt and perform a dynamic Monte Carlo (MC) simulation.[20,52,53] There are a number of intrinsic advantages as well as disadvantages to this approach; we discuss each in turn.

A dynamic MC simulation consists of the random sampling of configuration space by the following procedure.[52] Starting with an initial configuration of the system, one then chooses a chain at random and then a bead at random. One then randomly displaces, by a set of elemental local moves, the bead of interest. One must be careful that the choice of allowed moves spans the configuration space of the chains, otherwise nonphysical dynamics will result.[22,54-56] In the case of systems interacting solely with a hard-core

potential, the move is accepted, provided that two or more beads do not overlap. This method of sampling is known as an asymmetric Metropolis MC scheme. Provided that some additional assumptions are fulfilled, in particular that there must be a path to every state on the system and every step of the process is reversible, then in the limit of a large number of such micromodifications, the system will sample all states with a frequency that is close to their relative Boltzmann probabilities; thus good equilibrium sampling can be obtained.[52,53]

The asymmetric Metropolis MC scheme, when implemented using small-scale local micromodifications of the chain configuration, generates a solution to a stochastic kinetics master equation for the time evolution of the system and, therefore, is able to mimic dynamics.[57] Whether or not the dynamics is physical will depend on the kinds of moves employed. Care must be taken to make the elemental moves as small as possible to avoid the problem of significant time scale distortion. However, there is no guarantee *a priori* that the chosen moves can mimic physical dynamics. Checks must be performed, such as demonstrating that isolated random coil chains obey Rouse dynamics, that the scaling behavior of D and τ_R with n is recovered, and that the relative mobility exhibited by different chain topologies (e.g., rings and linear chains) tracks experiment.

The advantage of Monte Carlo dynamics (MCD), by setting the fundamental time scale as that required for local conformational modifications, is that it is inherently more efficient than molecular dynamics where the intrinsic time scale is associated with rattling about in local conformational wells. Thus, if one is interested in global relaxation properties of long-chain polymers where presumably such details are unimportant, then MCD is the method of choice.

MCD can, in principle, be performed both on[53,58] and off lattice.[20,21] The advantage of performing MCD on the lattice is twofold. First of all, it allows one to perform the calculations in integer arithmetic, therefore, providing at least an order of magnitude speed up over off-lattice calculations that must be done using floating-point arithmetic. Second, it allows one to rigorously insure that no bond cutting occurs. By use of a lattice occupancy list, this can be done extremely efficiently.[23] Since entangled systems are the object of these studies, it is extremely important that the only way entanglements relax is through physical processes, and not by the nonphysical passing of one chain through the other. The disadvantage is that one is confined to a lattice, and one must show that the results are consistent with off-lattice simulations and that the qualitative results of the simulation are not lattice artifacts. This is always a concern when performing lattice calculations.

In what follows next we present an overview of the results of the diamond[23] and cubic lattice[47,48,59] MCD simulations performed over the past several

years by Kolinski, Skolnick, and co-workers for melts of linear and ring polymers; the former simulations are discussed first. As in all simulations of this genre that were previously performed on much smaller systems,[56,60-62] the lattice is enclosed in a periodic box of size $L \times L \times L$. To avoid the problem of a given chain interacting with its periodic image, L is chosen such that it is larger than the root-mean-square end-to-end vector $\langle R^2 \rangle^{1/2}$.[23,48,49] Each polymer chain occupies n lattice sites, and ϕ is the volume fraction of occupied sites. The dynamic properties of homopolymeric (i.e., a melt in which all the chains are equal in length and identical in composition) diamond lattice polymers[23] were examined over a range of volume fraction ϕ from an isolated chain to $\phi = 0.75$, and n ranged up to 216. The cubic lattice polymers were studied at fixed $\phi = 0.5$, for a range of chain lengths $n = 64$ to 800 for the homopolymeric melt.[48]

The first problem one must address, before undertaking the simulation of the dynamics, is the construction of a dense equilibrated melt. The details for preparing such systems has been discussed at length elsewhere.[63] Then one must choose the set of local moves; the importance of this has been discussed above.[54-56]

The local elemental moves that are employed must not only have the ability to diffuse orientations down the chain, but just as in the real system, the ability to introduce locally new orientations into the chain interior as well.[54,55] For the case of diamond and cubic lattices, the set of elemental moves depicted in

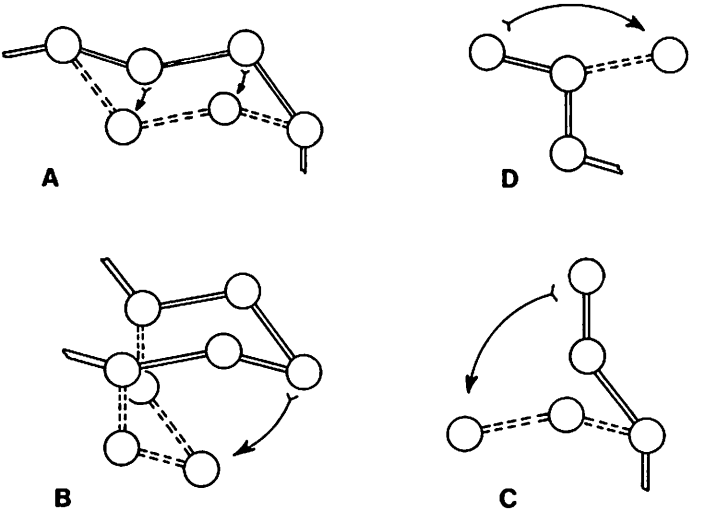

Figure 2. Elementary conformational modifications for diamond lattice polymers. (*A*) Three-bond kink motion. (*B*) Four-bond kink motion. (*C*) One- and (*D*) Two-bond end motion.

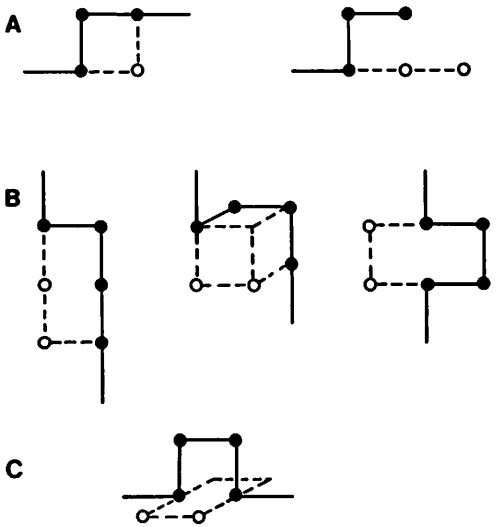

Figure 3. Elementary conformational modifications for cubic lattice polymers. (*A*) Two-bond kink motion and an example of chain-end motion. (*B*) Examples of three-bond kink motions. (*C*) An example of 90° crankshaft motion.

Figs. 2 and 3, respectively, satisfy these criteria.[23,47,48,56,58,62,64] The fundamental time unit is that when each of the beads, on average, is subjected to all the local motions. With this definition of time, the local moves shown in Figs. 2 and 3 give the correct isolated random coil (Rouse) dynamics. As shown below, it is encouraging that in spite of the very different local moves, both the cubic and diamond lattices exhibit the same qualitative behavior, when corrected for differences in local persistence length and lattice coordination number, thereby providing encouragement that the simulation results are physically meaningful.[23,48,49]

1. *Center-of-Mass Motion and Longest Internal Relaxation Times*

Before even beginning a detailed analysis of the internal chain motion, one must be sure that the scaling behavior of the self-diffusion constant and the terminal relaxation time are consistent with experiment. Figure 4*A* shows, in a log–log plot, the mean square displacement of the center of mass $g_{cm}(t)$ versus time for homopolymeric cubic lattice systems at $\phi = 0.5$.[47] Two distinct time regimes are apparent. For distances such that $g_{cm}(t) < 2\langle S^2 \rangle$, $g_{cm}(t) \sim t^a$ with a decreasing monotonically from 0.91 when $n = 64$ to 0.71 when $n = 800$. Qualitatively identical behavior is found on the diamond lattice[23] as well as in off-lattice simulations.[21] Hence the existence of a t^a regime with $a < 1$ is

not a lattice artifact, but is indicative of some kind of constrained dynamics where the center-of-mass motion couples into the internal relaxation processes. This is also consistent with the fact that $2\langle S^2 \rangle$ is the maximum distance over which the internal modes of an individual chain can relax if, in fact, the chains are statistically independent. Clearly then, the behavior of the longer chains is not Rouse-like (see Section I.C).

From the long time slope of the curve shown in Fig. 4*A*, the diffusion coefficient has been extracted. Fitting the data from $n = 64$ to $n = 216$, one finds a scaling behavior $D \sim n^{-1.52}$. At the time the simulations were done, we lacked the resources to run the $n = 800$ system into the free diffusion limit. Thus a number of extrapolation procedures were employed to extract the power law behavior of D; these are discussed elsewhere.[47] Here we quote the conclusion that the $n = 800$ system is well into the $D \sim n^{-2}$ regime.

The next quantity examined is the longest internal relaxation time τ_R, obtained by standard techniques from the decay of the autocorrelation function of the end-to-end vector. Table I summarizes the scaling of $D \sim (n-1)^{-\alpha}$ and $\tau_R \sim (n-1)^{\beta}$ for the diamond and cubic lattice systems.[23,48] In the case of diamond lattice systems, the deviation in α and β from $\alpha = 2$ and $\beta = 3.4$ arises at lower density from the fact that the chains studied are not long enough to cross over to entangled behavior. Increasing the density at fixed chain length increases the extent of interchain entanglement. For example, the longest chains simulated at $\phi = 0.5$ on the diamond lattice are $n = 216$. This roughly corresponds to a $n = 100$ chain on the cubic lattice, since chains on a diamond lattice are inherently stiffer. Thus longer chain lengths would have to be simulated to observe the asymptotic scaling behavior. Note that the $\phi = 0.75$ chains on the diamond lattice exhibit the requisite scaling.[23] These systems are highly mobile, and no evidence of the slowing down for distances greater than a bond length, indicative of the onset of the glass transition (which does occur at $\phi = 0.92$),[63] is seen. These chains exhibit globally isotropic long-time behavior. Thus the range of densities and chain lengths are appropriate to examine the existence of reptation, since $\alpha = 2.05$ and $\beta = 3.36$, the desired scaling with chain length is found.

Note that at all concentrations the product $D\tau_R$ scales like $n^{1.2}$ for a diamond lattice independent of the concentration[23] and $n^{1.1}$ for the cubic lattice.[47] Based on elementary scaling arguments, $D\tau_R$ should scale like $\langle S^2 \rangle$, which is proportional to $n^{1.0}$.[37] Perhaps this reflects the ± 0.05 uncertainties in the exponents α and β at high densities, or perhaps this is due to the conjectured crossover regime before $D\tau_R \sim n^{1.0}$. The Colby et al.[37] measurements are not inconsistent with this explanation, but they by no means demand it. A third explanation is to take the observation at face value and conclude that $D\tau_R \sim n^{1+\varepsilon}$ with $\varepsilon > 0$. This idea forms the basis of a theory of polymer dynamics introduced by Fixman[18,19] (see Section III.D).

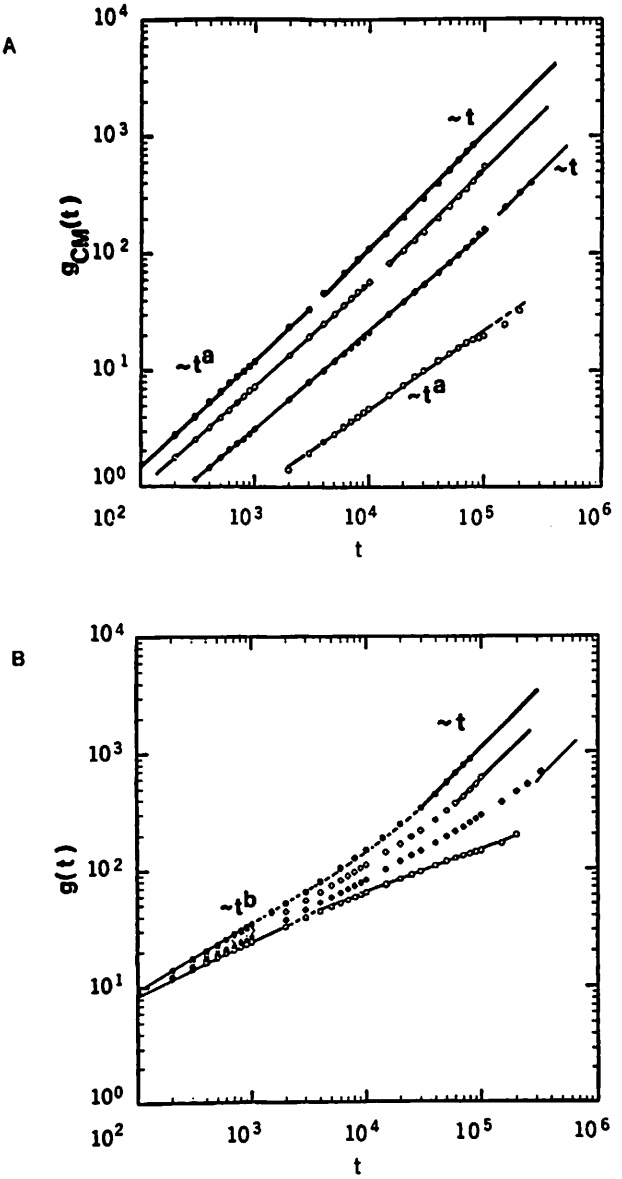

Figure 4. For homopolymeric cubic lattice polymers at $\phi = 0.5$, plot of the mean square displacement of the center of mass, $g_{cm}(t)$ vs. time in (*A*) and the average single bead displacement $g(t)$ vs. time in (*B*).

TABLE I
Chain Length Dependence of the Self-Diffusion Coefficient $D \sim (n-1)^{-a}$ and the Terminal Relaxation Time, $\tau_R \sim (n-1)^b$ on Cubic and Diamond Lattices

ϕ	a	b
	Cubic Lattice	
0.5	1.52 (±0.006)	2.63 (±0.04)
	Diamond Lattice	
Single chain	1.154 (±0.010)[a]	2.349 (±0.018)[a]
0.25	1.372 (±0.021)[a]	2.563 (±0.061)[a]
0.50	1.567 (±0.017)[a]	2.677 (±0.035)[a]
0.75	2.055 (±0.016)[a]	3.364 (±0.082)[a]

[a] Standard deviation of the slope obtained from linear least-square fit of log–log plots.

Next, the finer details of the chain dynamics will be examined. In Fig. 4*B*, the average mean square displacement per bead, $g(t)$, is plotted versus time on a log–log plot for the $\phi = 0.5$ cubic lattice chains.[47] Just as for $g_{cm}(t)$, two distinct time regimes are evident. The first regime, which once again extends up to $2\langle S^2 \rangle$, exhibits a $g(t) \sim t^b$ dependence, where b decreases gradually from the Rouse exponent value of 0.54 when $n = 64$ to a value of 0.48 when $n = 216$. If one stopped increasing the length of the chains at this point, one might reasonably conclude that the dynamics of these chains is entirely Rouse-like. However, this doesn't hold for the $n = 800$ system. Here there is a region where $g(t) \sim t^{0.36}$, once again indicative of the more constrained nature of the dynamics of these chains.

It is not unreasonable to guess that the behavior exhibited by $g(t)$ and $g_{cm}(t)$ is indicative of the crossover to reptation dynamics where one expects a $g(t) \sim t^{1/4}$ regime (see Eq. 8). One might expect that the central beads of the chain would cross over to the $t^{1/4}$ regime first. Thus Figs. 5*A* and *B* present log–log plots of the average mean-square displacement of the central five beads in the chain $g_5(t)$ versus t for $n = 216$ and $n = 800$ chains, respectively. There is clear evidence for a $t^{1/4}$ regime. The fundamental question still remains; namely, are these chains reptating? To get slightly ahead of the story, as shown in the next section, a detailed microscopic analysis of the microscopic motions of these chains indicates that the character of the chain motion is entirely different.

In fact, the existence of a $t^{1/4}$ regime is indicative of some sort of constrained interchain dynamics and is *not a unique signature of reptation.* This statement is further substantiated by a recent simulation of Milik et al.[65] on a model of a membrane, confined to a diamond lattice. The head of each molecule is constrained to bob up and down, no more than one lattice unit in the z

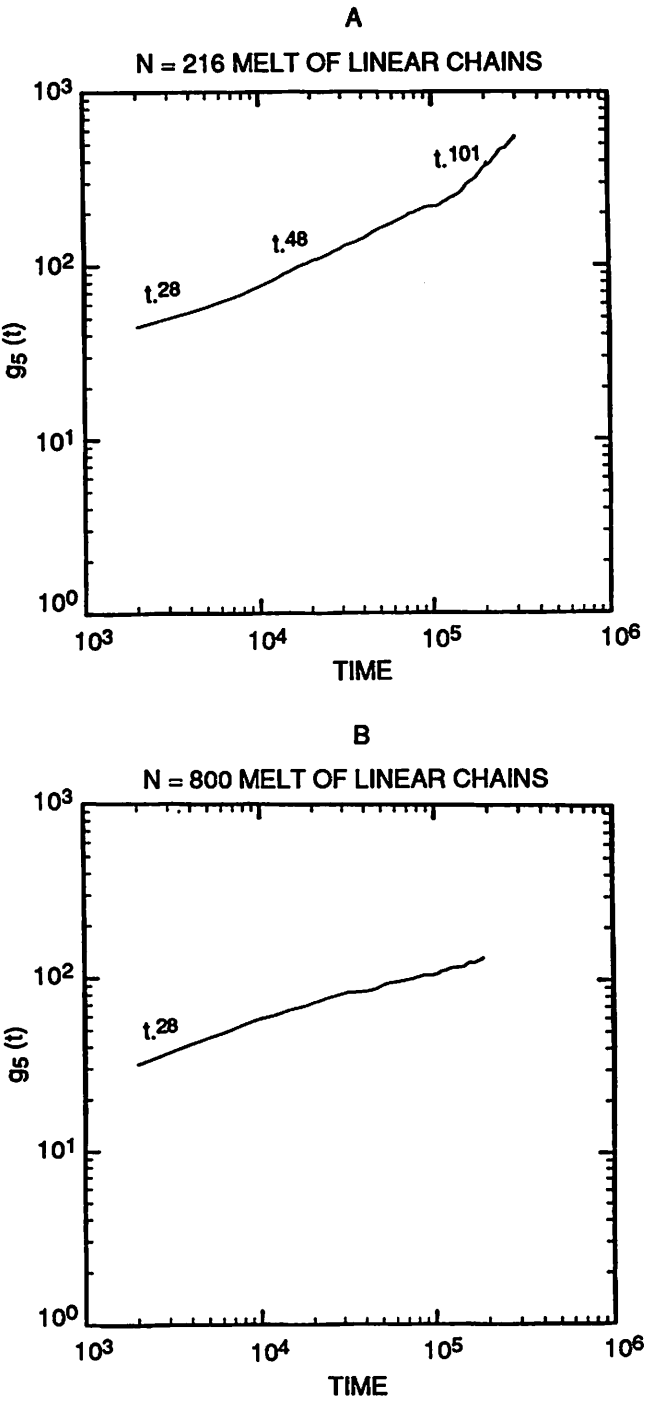

Figure 5. Plot of the mean square displacement of the central five beads, $g_5(t)$ vs. time for $n = 216$ (A) and $n = 800$ (B) in $\phi = 0.5$, homopolymeric, cubic lattice melts.

direction, but the chains are free to move in the other two dimensions. Given the constraints on the dynamics, these chains cannot possibly reptate (one tail is more or less nailed down in one dimension). There is the standard $t^{1/2}$ regime; this is followed by a $t^{1/4}$ regime at distances corresponding to the mean spacing between chains. Hence the existence of a $t^{1/4}$ regime in the single bead autocorrelation function does not prove the existence of reptation, since systems which cannot possibly reptate exhibit this behavior as well.

2. *Examination of the Primitive Path Dynamics*

In their classic papers developing many of the essential ideas of the reptation model, Doi and Edwards[5-8] invoke the idea of a primitive chain path.[66] The primitive path entails the replacement of the actual chain by an equivalent in which all the local fluctuations in the chain contour which are irrelevant to the long distance motion are averaged out. Conceptually, this is much like taking the original chain contour, reeling in the slack, and examining the resulting path.

To examine the trajectories of the chains in the simulation, we have constructed an equivalent chain and followed its motion as a function of time.[23,47,48] The outline of the procedure is as follows: Each bead in the original chain is replaced by a point on the equivalent chain which is the center of mass of a subchain composed of n_b beads. This replaces the actual chain contour by a smooth path of partially overlapping subchains, which should be a good approximation to the primitive path of Doi and Edwards if n_b is on the order of the number of monomers between entanglements. (Actually, the results described below are quite insensitive to n_b.) The equivalent path is generated as a function of time. At every time the equivalent path is projected onto the original path defined at zero time. The displacement down the original path corresponds to the reptation component. What remains is the nonreptation component of the dynamics, which should be small if reptation is dominant.

To quantify the measurement of reptation, the mean-square displacements down the original primitive path, $g_{\parallel}(t)$, and perpendicular to the original primitive path, $g_{\perp}(t)$, are calculated. If the chain reptates, it is straightforward to show that the maximum value of $g_{\perp}(t)$ equals one-half the mean-square tube radius for times less than the tube renewal time.[23] Thus the ratio $g_{\perp}(t)/g_{\parallel}(t)$ should monotonically decrease with increasing time. If, however, the motion is isotropic and liquid-like with little if any memory of a tube defined at zero time, then $g_{\perp}(t)/g_{\parallel}(t)$ should monotonically increase. Thus, examining this ratio is a nonbiased way of directly addressing the question of whether or not a given system of chains reptates in a fixed tube. It is interesting to point out that reptation theory assumes that a kind of glass transition is occurring in the melt. That is, the motion of the chain perpendicular to the original path is essentially frozen out due to the existence of entanglements.

Since the simulations involve MCD on a lattice, it is important to establish that somehow reptation is not artificially suppressed by the choice of elemental moves and to verify that the ratio $g_\perp(t)/g_\parallel(t)$ does indeed indicate reptation when in fact it is present. It is well established that if a single chain is confined to a fixed mesh and if it is sufficiently long, the chains will reptate.[21,43,44]

To validate the simulation methodology, we examined the dynamics of a single chain in a partially frozen environment.[23] Basically, what one does is take the original $n = 216$ diamond lattice polymer $\phi = 0.5$ melt, and freezes all but one test chain in place. However, if all the matrix chains are completely frozen, since the tube is not porous, the test chain is trapped. Thus a partially frozen environment was employed, where every eighteenth bead in the matrix chains is frozen in place. This allows for local dynamics that are quite close to the original melt, but where all the chains but the test chain are constrained from moving appreciable distances.

Examination of the primitive path revealed that the chains reptate and the ratio $g_\perp(t)/g_\parallel(t)$ versus time monotonically decreases, as expected.[23] The signature of reptation is recovered, and one finds the expected presence of reptation. Hence the MCD moves that are used do not somehow artificially suppress reptation. We do note, however, that there is substantial tube leakage,[1] with loops running up and down cul de sacs. A further interesting point, that is not surprising, is that the chain in the partially frozen environment moves substantially slower than when all the chains are free to move.

In Fig. 6 the ratio $g_\perp(t)/g_\parallel(t)$ versus t is shown for the cubic lattice melt,[47] where everything moves, for chains with $n = 216$ and $n = 800$. Here n_b has been set equal to 17 as well as 101, and no qualitative difference is found.

The qualitative features exhibited in Fig. 6 are identical to those seen for chains on the diamond lattice.[23] At short times transverse motion of the chains is preferred. This results from the nature of cooperative motions at high density, whose origin is as follows.[63] Imagine a chain has undergone a conformational rearrangement. The probability of the chain undergoing correlated motion is the product of two quantities: (1) the intrinsic probability that the chain is in a conformation in which a conformational change is possible and (2) the probability that there are unoccupied sites, into which the chain can jump. For both cross- and down-chain motion, the intrinsic probabilities are identical. However, for cross-chain motion, given that the chain has already undergone a jump, there is now an unoccupied volume that the neighboring chain can jump into. The conditional probability that the neighbor can undergo the jump is unity. In the case of down-chain motion, this probability is to lowest order proportional (on a lattice) to $(1 - \phi)$ raised to the power of the number of sites involved in the motional unit. Therefore, with an increase in density, one would expect that cross-chain motion is dominant at short

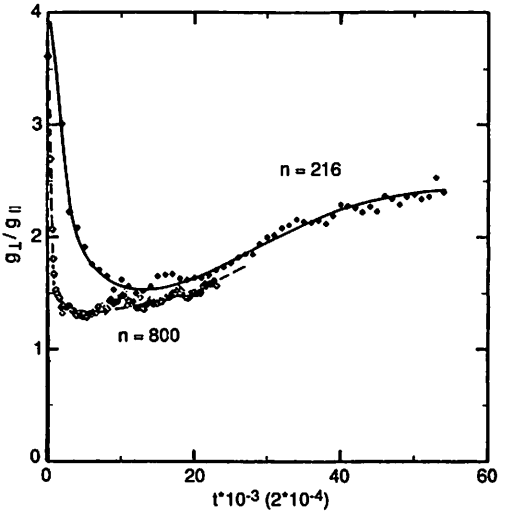

Figure 6. Plot of the ratio $g_\perp(t)/g_\parallel(t)$ vs. time $\times 10^{-3}$ (2×10^{-4}) for $n = 216$ (800) in the upper (lower) curve. Both are at a density of $\phi = 0.5$ on a cubic lattice.

times, as is observed. This qualitative conclusion is independent of whether or not the chains are on a lattice.

Subsequent to the short time preference for transverse motion, there is a period when down-chain motion becomes more important. This corresponds to distances on the order of the excluded volume decay length. For these distances, the chain starts to feel the effect of the environmental constraints and has slowed down. There is a certain incubation period before the collective motion of the chains that gives rise to the lateral motion takes over. Finally, at longer times the reptation component becomes less important and the lateral component grows. In fact, it becomes increasing difficult to follow the original primitive path and project on it. This is true, in spite of the fact that according to reptation theory this is precisely the distance and time regime for which reptation dynamics should be very well defined.[1,4-8,37] Note that we have only examined the primitive path for the middle third of the chain, because any chain, whether reptating or not, undergoes substantial fluctuations of the ends.[17,23]

An interesting point observed on comparison of Fig. 6 with Fig. 5*A* and *B* is that the minimum in $g_\perp(t)/g_\parallel(t)$ versus t occurs just as the chains are crossing out of the $t^{1/4}$ regime in the $g_5(t)$ versus t plot. Thus if one were to merely look at $g_\perp(t)/g_\parallel(t)$ for times just up to the end of the $t^{1/4}$ regime, but for motion over distances still small relative to the radius of gyration, one would incorrectly

conclude that reptation is quite important. It is not until the chain goes further into the second $t^{1/2}$ regime that reptation becomes a minor component of the dynamics. Thus a recent off-lattice molecular dynamics simulation,[24] which claims to see reptation, is in fact, inconclusive because only times up to the end of the $t^{1/4}$ regime are sampled. The simulation times are too short to demonstrate whether the chains are reptating or not. As discussed above, the existence of a $t^{1/4}$ regime in $g(t)$ versus t plots is insufficient to prove the existence of reptation. *Other modes of cooperative dynamics give this result as well.*

A more pictorial illustration of the character of chain motion is shown in Fig. 7*A–C*, where the trajectory of one of the $n = 800$ chains confined to a cubic lattice is presented. The thin line corresponds to the conformation at the initial time, and the thicker line shows the conformation at a time t, later. The triangle indicates the position of one of the chain ends. For ease of visualization, n_b was set equal to 101. Consistent with the ratios $g_\perp(t)/g_\parallel(t)$ versus t, substantial lateral fluctuations are evident. One is forced to conclude that these chains, at least, do not know that they are confined to a static tube.

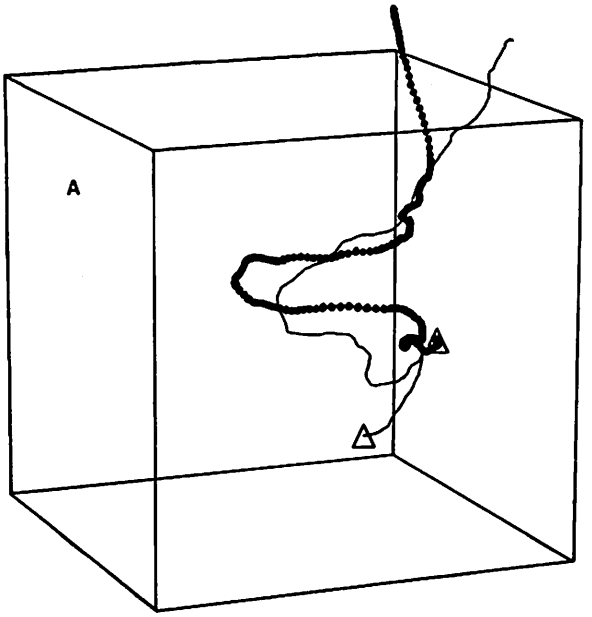

Figure 7. (*A–C*) Snapshot projections of the primitive path of a chain of $n = 800$ in the $\phi = 0.5$ cubic lattice melt. The thin line corresponds to the initial conformation and the triangle labels one of the ends. The displacement after 6×10^4 steps, 1.2×10^5 steps, and 2.0×10^5 steps is shown in *A–C* respectively.

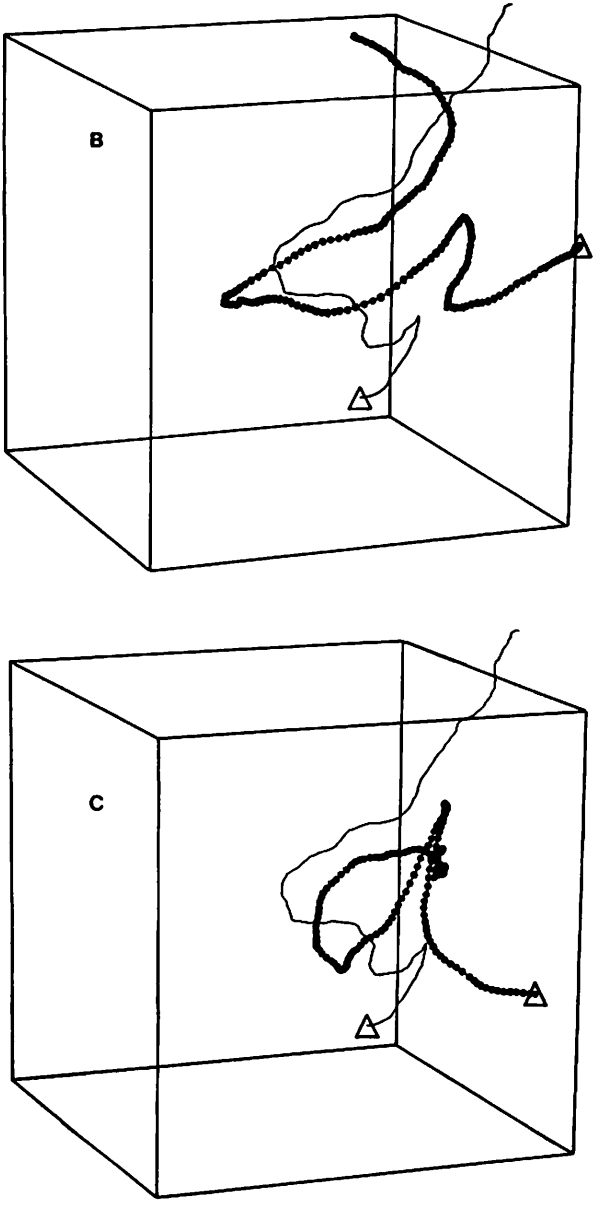

Figure 7. *(Continued)*

The question still remains as to whether or not real chains reptate. Certainly, these simulations strongly argue against the existence of a fixed tube, but it could be argued that these chains are in the crossover regime from Rouse to reptation dynamics. In this regime, one might still expect substantial tube fluctuations; in other words, we are observing a regime where the chains do not *yet* reptate. Since the $n = 800$ chains are about at the limit of our computational capabilities, we cannot rule out a crossover to fixed-tube/reptation behavior at increased chain length. However, because the present simulations reproduce the experimental scaling of D and τ_R, it would have to be a crossover from a regime where classical reptation is not dominant to a regime where reptation dominates which is invisible to experiment, at least via the standard techniques that have been employed.

B. Probe Polymer in Matrices of Different Molecular Weight

Another important observation is that when a test or probe polymer is dissolved in a matrix of polymers of identical chemical composition but increasing molecular weight, the diffusion constant of the probe, D_p, becomes independent of matrix molecular weight.[28,29,67] To examine whether the present model system could reproduce this behavior, the dynamics of a probe chain composed of $n_p = 100$ segments in matrices from $n_m = 50$ to 800 segments was explored in a cubic lattice system having $\phi = 0.5$.[48] Over this range of matrix molecular weights, the diffusion constant of the probe decreases by approximately 30%; this is consistent with the decrease in D_p observed in real experiments.[27] While a chain of $n_p = 100$ is not sufficiently long to have crossed over into the n^{-2} regime of the diffusion constant, the probe in the $n_m = 800$ system had a diffusion constant that is two orders of magnitude larger than the matrix in which it was dissolved.

The primitive path analysis clearly showed that the motion of the chain is not confined to a tube and that the motion is not reptation-like. Otherwise stated, the local fluctuations in the topological constraints imposed by the matrix are sufficiently large even for the $n_m = 800$ case to allow for essentially isotropic, but somewhat slowed-down, motion of the probe chains in the melt. Thus the MCD is once again in qualitative accord with experiment, and yet reptation within a confining tube is not found.

C. MCD Simulation of Melts of Rings

More recently, Sikorski, Kolinski, Skolnick, and Yaris[59,68] undertook a series of simulations designed to examine the nature of the dynamics of a melt of uncatenated rings; two distinct physical cases were examined. The first, and simplest, involved a cubic lattice melt of unknotted cubic lattice rings, packed at a volume fraction $\phi = 0.5$; a range of chain lengths from $n = 100$ to 1536 was studied. The second case involved the dynamics of a melt of rings

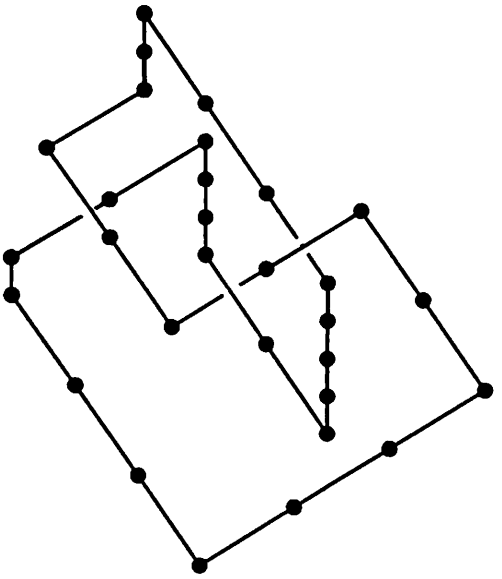

Figure 8. Conformation of an $n = 30$ ring on a cubic lattice containing one self-knot.

containing one self knot, such as is shown in Fig. 8. The motivation of this simulation, suggested to us by McKenna, is as follows. Owing to the nature of the synthesis conditions, it is possible that real ring polymers might contain self knots, and the question arises as to whether such knots will drastically change the dynamic properties of a melt of rings.[39]

1. *Growth of Melts of Rings*

Just as in the linear case, one has to start with an equilibrated melt of rings before one can even begin to perform the dynamics. Recently, Pakula and Geyler developed a very efficient method for generating such a system on a fully occupied lattice.[69-71] This novel algorithm will be elaborated on in detail in Section II.E, where their simulation technique and results are more fully explored. Here we describe an algorithm for generating systems, in principle of arbitrary polydispersity, which should be quite efficient, provided that the density of the system is not too large.

As schematically depicted in Fig. 9 for the case of unknotted rings, one starts with a set of the smallest size rings, each containing four beads. One chain is shown for the sake of clarity; actually, N chains are simultaneously subjected to the growth/equilibration algorithm. These are then randomly grown and modified, just as is done for linear chains. However, unlike the

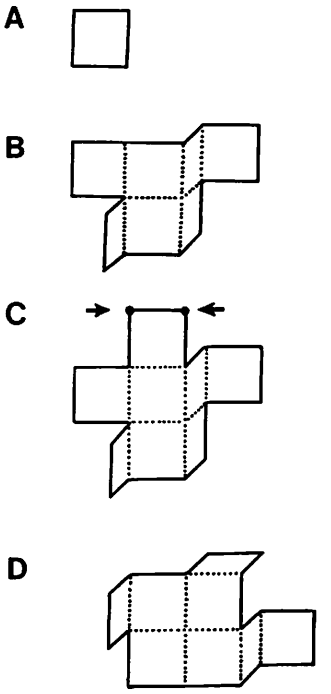

Figure 9. Schematic representation of the ring growth algorithm. One ring is shown for clarity. In reality all rings are simultaneously grown and equilibrated.

linear case,[63] reptation dynamics is useless (there are no free ends to randomly cut and paste). Fortunately, since rings are characterized by smaller chain dimensions and for isolated chains, at least, smaller relaxation times, this doesn't pose too severe a problem. That is, the systems can be run for sufficiently long times to be reasonably sure that equilibrated systems have been prepared. The rings undergo the same set of internal modifications as the linear chains shown in Fig. 3, with the exception that end moves are not performed. The process of growth/equilibration stops when all the rings are of size n. In principle, polydisperse melts of rings could be grown.

The advantage of this particular ring preparation procedure is that owing to the set of elementary jumps of MCD and the ring growth mechanism the rings cannot be catenated. Depending on the degree of polymerization and density, the rings can be rather highly entangled. Provided that the equilibration period between intervening growth steps is sufficiently long, the resulting system should be close to an equilibrated system. Following system preparation, the system is allowed to run for several relaxation times before sampling for the dynamic properties begins.

The only difference between growing rings that have no knots and rings with a single knot is in the starting conformation. Initially, rings having a single knot are placed in the box, and then they are subjected to the growth/equilibration process. Again, because of the bond pair insertion constraint that does not violate excluded volume, a monodisperse collection of rings, having one self-knot, can be generated as well.

2. *Equilibrium Properties*

To date, only two simulations of the equilibrium properties of a melt of rings have been undertaken, one by Pakula and Geyler[71] for rings on a fully filled cubic lattice, up to $n = 512$, and the present simulation for rings at $\phi = 0.5$, for rings up to $n = 1536$.[59,68] Qualitatively, identical behavior is observed. Before presenting the simulation results, it is appropriate to compare the expected scaling relationships of the conformational properties with the corresponding linear chains, if the statistics are Gaussian.[42] The mean square radius of gyration of the corresponding ring and linear chain of identical n are related by

$$\langle S^2 \rangle_{\text{ring}} = \langle S^2 \rangle_{\text{linear}}/2 \sim n^{1.0}, \tag{9a}$$

and the mean square diameter, which is the mean square distance between beads 1 and $n/2$, $\langle d^2 \rangle_{\text{ring}}$, is related to $\langle R^2 \rangle_{\text{linear}}$ by

$$\langle d^2 \rangle_{\text{ring}} = \langle R^2 \rangle_{\text{linear}}/4 \sim n^{1.0}. \tag{9b}$$

Combining Eqs. 9a and 9b,

$$\langle S^2 \rangle_{\text{ring}}/\langle d^2 \rangle_{\text{ring}} = \tfrac{1}{3}. \tag{9c}$$

These results are to be compared with the Pakula and Geyler[71] simulation result that

$$\langle S^2 \rangle_{\text{ring}} \sim n^{0.90}, \tag{10a}$$

and

$$\langle R^2 \rangle_{\text{linear}} \sim n^{1.006}, \tag{10b}$$

the latter holding for chains up to $n = 512$.

The Sikorski et al. result[59,68] is

$$\langle S^2 \rangle_{\text{ring}} \sim n^{0.84}, \tag{11a}$$

and

TABLE II
Equilibrium Statistics of Melts of Rings at $\phi = 0.5$

n	N	$\langle d^2 \rangle$	$\langle S^2 \rangle$	$\langle S^2 \rangle / \langle d^2 \rangle$	$\langle d^4 \rangle / \langle d^2 \rangle^2$	$\langle S^4 \rangle / \langle S^2 \rangle^2$	$\langle d^2 \rangle_{ring} / \langle R^2 \rangle$ lin[b]	$\langle S^2 \rangle_{ring} / \langle S^2 \rangle_{lin}$
100	20	46.9 ± 0.04	15.15 ± 0.07	0.323	1.540 ± 0.008	1.070 ± 0.002	0.250	0.492
100[a]	20	28.0 ± 0.8	11.60 + 0.02	0.414	1.666 ± 0.02	1.041 ± 0.001	0.149	0.377
216	24	91.8 ± 0.3	30.0 ± 0.3	0.336	1.587 ± 0.017	1.081 ± 0.003	0.222	0.458
392	28	154.6 ± 7.9	52.8 ± 1.4	0.342	1.597 ± 0.026	1.083 ± 0.006	0.215	0.424
392[a]	28	132.5 ± 10.0	45.4 ± 1.7	0.347	1.664 ± 0.020	1.084 ± 0.009	0.184	0.369
800	40	278 ± 19	95.2 ± 3.0	0.341	1.625 ± 0.077	1.091 ± 0.020	0.195	0.368
1536	40	469 ± 50	168.4 ± 5.6	0.359	1.657 ± 0.101	1.109 ± 0.020	0.169	0.333

[a] Melt of rings each containing one self knot.
[b] lin is the value for the linear system.

$$\langle d^2 \rangle_{\text{ring}} \sim n^{0.87}, \tag{11b}$$

which should be compared to the linear melt values[47] of

$$\langle R^2 \rangle_{\text{linear}} \sim n^{0.99}, \tag{12a}$$

and

$$\langle S^2 \rangle_{\text{linear}} \sim n^{1.02}. \tag{12b}$$

Thus the $\phi = 0.5$ result is in excellent agreement with the $\phi = 1.0$ result of Pakula and Geyler.[71] With respect to the equilibrium properties at least, the $\phi = 0.5$ system is essentially identical in scaling behavior to the fully occupied lattice system.

In Table II, the Sikorski et al. equilibrium results[59,68] are summarized for both the unknotted system and the system having one self knot. The latter systems, not unexpectedly, have smaller dimensions than the unknotted rings, but the relative difference between the two cases decreases with increasing chain length.

The simulation results of both groups are in reasonable agreement with the Flory-like mean field treatment of Cates and Deutsch,[72] which gives

$$\langle d^2 \rangle_{\text{rings}} \sim n^{4/5} \tag{13}$$

in three dimensions. The crux of their argument is as follows. If excluded volume interactions are fully screened, the fact that catenated ring conformations are prohibited exerts a topological constraint on the system, and the more extended the conformation is, the greater is the topological constraint. Thus rings in a melt should tend to collapse. Opposing this is the Gaussian entropic force. Equation (13) results from minimizing the free energy due to these two competing effects, with the result that rings are less expanded than would be predicted from Gaussian statistics alone.

One of the more interesting and unexplained relationships of Table II is that while the $\langle S^2 \rangle_{\text{rings}}$ and $\langle d^2 \rangle_{\text{rings}}$ are distinctly non-Gaussian in behavior, their ratio is close to the Gaussian value of 1/3.

3. *Dynamic Properties of Unknotted Rings*

The procedure for extracting the self-diffusion coefficient and the longest relaxation time τ_d (which corresponds to the relaxation of the diameter autocorrelation function) is discussed elsewhere.[59,68] Values of D, τ_d, and a number of other dynamic quantities for rings of $n = 100$, 216, 392, 800, and 1536 are shown in Table III. Given the computational resources, we cannot carry out

TABLE III
Self-Diffusion Constant and Terminal Relaxation Times for $\phi = 0.5$ Melt of Rings

M	D	τ_d	$D\tau_d/\langle d^2 \rangle$	n/n_e[b]	a[c]	b[d]
100	1.14×10^{-3}	1.15×10^{3}	2.80×10^{-2}	0.20	0.96	0.61
100[a]	9.15×10^{-4}	1.17×10^{3}	3.82×10^{-2}		0.95	0.56
216	4.35×10^{-4}	7.50×10^{3}	3.55×10^{-2}	0.42	0.88	0.52
392	1.88×10^{-4}	3.02×10^{4}	3.67×10^{-2}	0.77	0.87	0.45
392[a]	2.85×10^{-4}	2.43×10^{4}	5.23×10^{-2}		0.90	0.46
800		1.43×10^{5}		1.57	0.85	0.46
1536		5.89×10^{5}		3.01	0.80	0.41

[a] Melt of rings each containing one self-knot.
[b] Estimated from Eq. (15a).
[c] Exponent of $g_{cm}(t) \sim t^a$ for distances less than $2\langle S^2 \rangle$.
[d] Exponent of $g(t) \sim t^b$ for distances less than $2\langle S^2 \rangle$.

the $n = 1536$ simulation into the free diffusion limit. The diffusion constant scales with n like

$$D \sim n^{-1.42}, \tag{14a}$$

and

$$\tau_d \sim n^{2.32}. \tag{14b}$$

This scaling behavior suggests that the rings are in the crossover regime and are not as entangled as the corresponding linear system.

Another means of estimating the number of entanglements follows from an analytically derived expression for the diffusion constant of a chain in the melt[16] (see Section III.B below)

$$D(n) = \frac{d_0}{n\left(1 + \dfrac{n}{n_e}\right)}, \tag{15a}$$

where n_e is the mean number of monomers between entanglements. Fitting this expression to data in Table III gives n_e (rings) = 515, and employing the analogous expression to fit the linear data[47,48] gives

$$n_e(\text{rings})/n_e(\text{linear}) = 3.9. \tag{15b}$$

In other words, the melt of rings is less entangled and therefore, more mobile than the corresponding melt of linear chains. This ratio compares quite favorably to the ratio of approximately 5 obtained for polybutadiene;[40] other

ratios reported for polystyrene are about two.[39] Hence the simulations once again reproduce the experimental trends.

Unfortunately, since rings have a larger n_e than the corresponding linear chains this means that it is presently impractical to simulate rings of a comparable (albeit relatively small) degree of entanglement as the corresponding linear chains on available computers. The decrease in the number of entanglements is partially due to the more compact dimensions of rings as

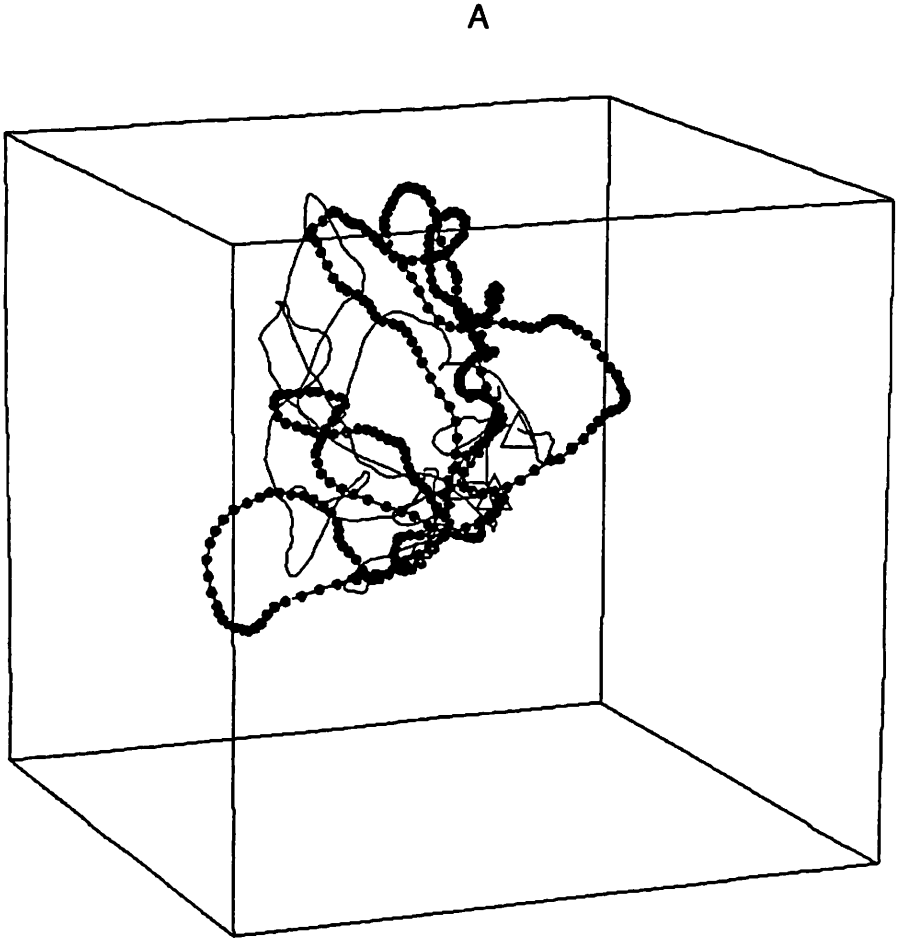

Figure 10. (*A–C*) Snapshots of the primitive path of an $n = 1536$ ring in the $\phi = 0.5$ cubic lattice melt. The thin line denotes the initial conformation, and the triangle labels beads 1 and 1536. The displacement after 3.04×10^5, 8×10^5, and 1.008×10^6 steps is shown in *A–C* respectively.

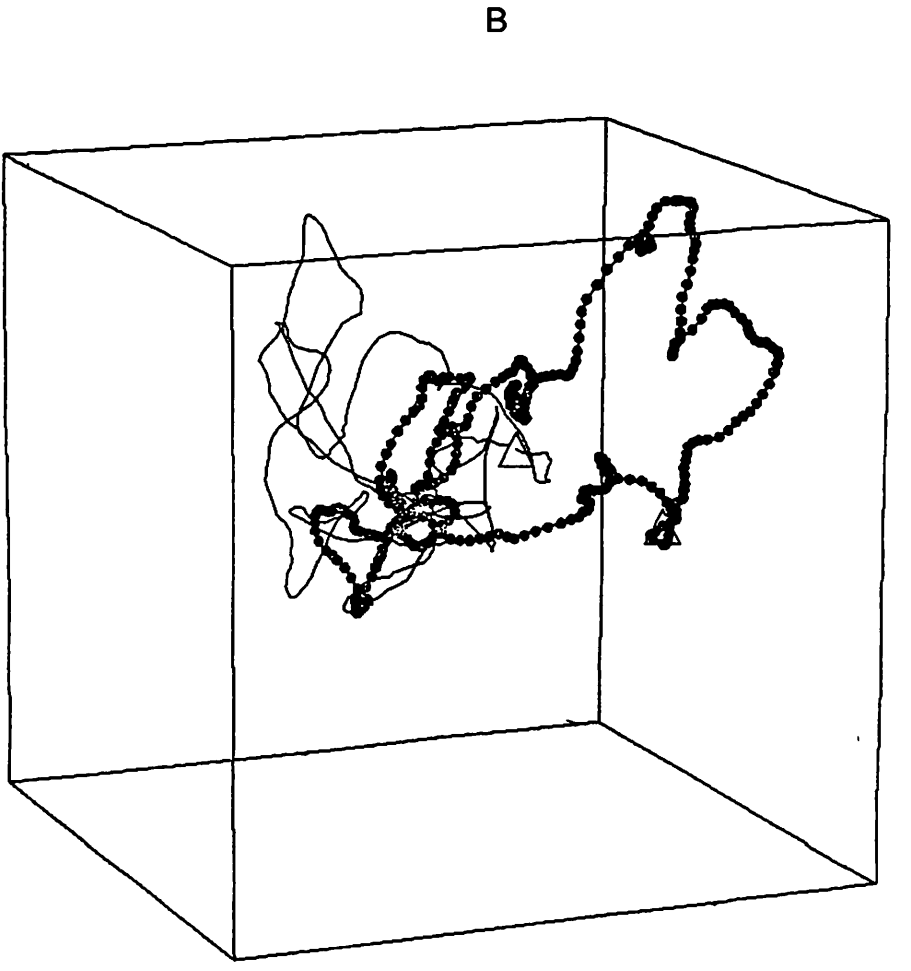

Figure 10. *(Continued)*

compared to the corresponding linear chains. Another effect may be due to the nature of the entanglements themselves, a point that we address further in the next section.

For advocates of reptation, rings being entirely devoid of ends pose a particular problem. Klein[38] has proposed a model which asserts that the only rings which are mobile are those that collapse to a linear chain of half the contour length. If this expectation is true, one would expect to find almost all rings immobile and an exponentially small subpopulation that is highly

C

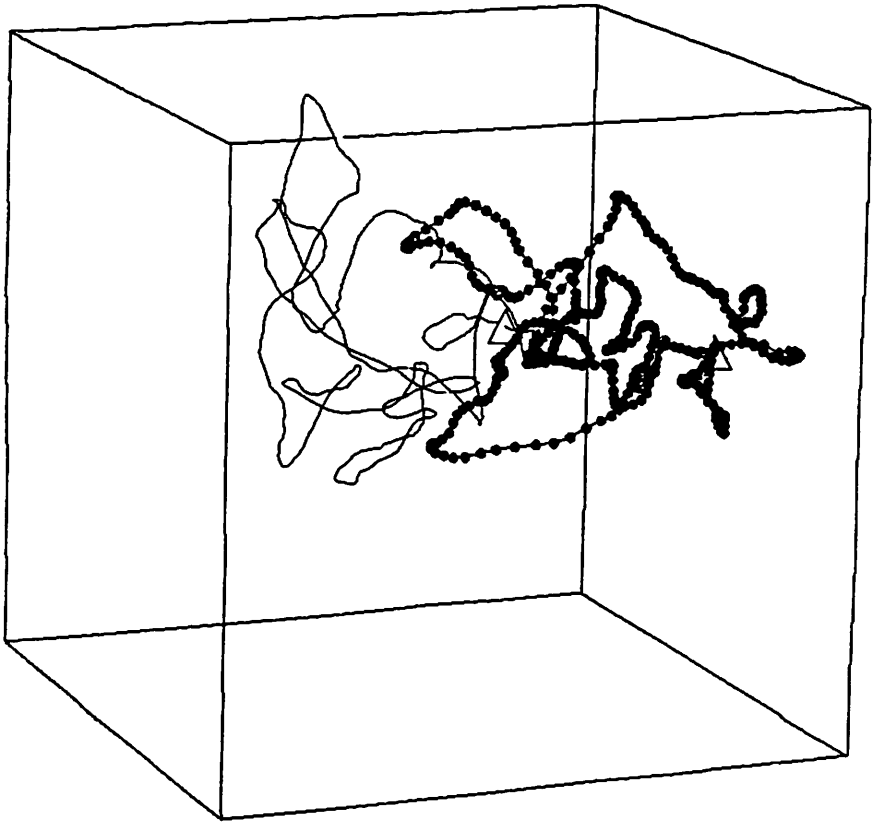

Figure 10. *(Continued)*

mobile. Thus we examined the population of mobile rings to see if such a bimodal population exists; none was found.

We next present the primitive path as a function of time for the $n = 1536$ system in Fig. 10*A–C*. The triangle labels beads 1 and 1536. The thin line indicates the initial primitive path obtained at zero time, and the solid line labels the path at a time t later. Nothing striking or reptation-like is seen—rather rings seem to move much like amoebas.

In all fairness to the advocates of reptation, these systems are weakly

entangled; nevertheless, if reptation were the dominant mechanism of melt dynamics, one would have expected the onset of reptation for rings to occur at smaller—and not larger—degrees of entanglement than in the corresponding linear chain case. However, because these systems are early in the crossover regime, a transition to much slower dynamics cannot be ruled out—although there is no hint of any such transition in the simulations performed thus far.

4. *Properties of Self-Knotted Rings*

We next turn to the behavior of the dynamics of a melt of rings, each containing one self knot. Care has to be taken when comparing the dynamics of self-knotted rings with unknotted rings because of an artifact of lattice dynamics. Consider a ring containing one self knot, the minimum ring size that can fit onto a cubic lattice contains 22 beads and is left absolutely immobile when subjected to the internal moves of Fig. 3. This is a close-packed object that can only undergo rigid body translations and/or rotations, and these have not been incorporated into the present MCD algorithm. Thus, one should expect two competing effects as n increases. First of all, internal conformational transitions become possible, and thus D increases from zero. This effect is as indicated above, an artifact of the MCD algorithm that is employed. Second, as polymeric effects take over, D should decrease with increasing molecular weight. Finally, D for isolated chains without knots should always be larger than D with knots (since the conformations of the latter are more compact). When comparing the results of the dynamics of knotted versus unknotted rings in the melt, one wants to be sure that artifacts are eliminated, and we therefore examine the dynamics of isolated rings first to be sure such artifacts are not present.

In the solid (open) circles of Fig. 11, results of D versus n for isolated rings containing one (no) self knot are shown on a log–log plot. Beyond $n = 100$, and certainly for n greater than or equal to 216, D for the knotted system is well defined and monotonically decreases with increasing n.

Fitting the log–log plot for $n = 216$, 800, and 1536, we find for the knotted system that

$$D \sim n^{-1.3}, \tag{16a}$$

and for the terminal relaxation fit over the range of $n \geq 100$ that

$$\tau_d \sim n^{2.2}. \tag{16b}$$

By way of comparison, the equilibrium quantities are

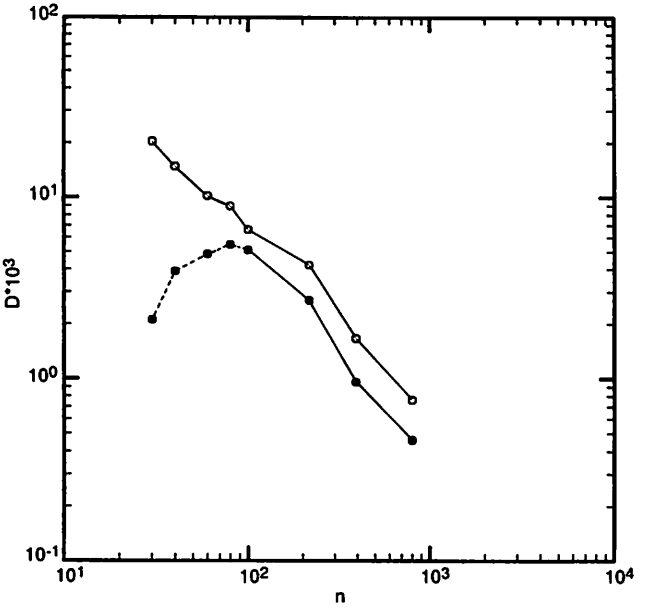

Figure 11. Log–log plot of the self-diffusion coefficient of isolated ring polymers confined to a cubic lattice vs. n. The solid (open) circles are for rings having one (no) self-knots.

$$\langle S^2 \rangle = 0.0411(n-1)^{1.28} \tag{16c}$$

and

$$\langle d^2 \rangle = 0.1090(n-1)^{1.28}. \tag{16d}$$

The corresponding quantities for the isolated unknotted rings, are for a fit over the range 30–1536,

$$D \sim n^{-0.96}, \tag{17a}$$

$$\tau_d \sim \mathrm{n}^{2.1}, \tag{17b}$$

$$\langle S^2 \rangle = 0.1079(n-1)^{1.16}, \tag{17c}$$

and

$$\langle d^2 \rangle = 0.3266(n-1)^{1.19}. \tag{17d}$$

Based on these results we can probably safely compare the dynamics of melts of self-knotted rings with those of unknotted rings for $n = 216$ or greater. Table III also presents a summary of the dynamic properties of melts of self-knotted rings of $n = 100$ and 392. Comparing the knotted with the unknotted rings, it is immediately apparent that within the error of the simulation the dynamics of a melt of self-knotted and unknotted rings are essentially identical. Probably because self-knotted rings are smaller (having $\langle S^2 \rangle$ of about 133 vs. $\langle S^2 \rangle$ of 155, for $n = 392$) than unknotted chains, the self-knotted rings are less entangled and, therefore, slightly more mobile (this competes with the intrinsically lower mobility of isolated self-knotted chains; the latter effect should be more important at smaller n, as is observed). Nevertheless, the effect is minor and we conclude that self knotting will have a marginal effect, at best, on the melt dynamics.

D. The Origin of Entanglements

Whatever the physical origin of the interchain entanglements, to exert an influence on the long distance motion, they must live for times on the order of the terminal relaxation time or perhaps longer. Otherwise, they can be subsumed into a molecular weight independent, monomeric friction coefficient and therefore, they wouldn't change the scaling with molecular weight of the transport coefficients. Based on the results for the linear chain simulations which in many, but not all, respects behave like slowed-down, Rouse chains,[23,47,48] one might conjecture that the slowdown in behavior results from dynamic entanglement contacts. That is, one chain drags another chain for times on the order of the terminal relaxation time. Eventually, of course, these entanglements should disengage. This is an old idea in the literature, which goes back to Bueche,[2,73] variants of which have been proposed by Fujita and Einaga[9,10], Ngai et al.,[14,74] Kolinski et al.,[16,17,23,47,48] and Fixman.[18,19] Thus we next examine what the simulations have to say about this conjecture.

1. *Bead Distribution Profiles*

In Fig. 12 the time dependence of the mean-square displacement of the ith bead $g_i(t)$ is plotted as a function of the position i, along the chain for $n = 216$ linear chains, packed at $\phi = 0.5$ diamond lattice melt.[23] In the curves denoted by a–d, the time equals 3×10^4, 6.9×10^5, 1.35×10^6, and 2.1×10^6 time steps ($\tau_R = 5.2 \times 10^5$). The smooth curves are generated by using the Rouse model and an apparent diffusion coefficient defined as $g_{cm}(t)/6t$. The Rouse model is seen to overestimate the mobility of the chain interior and underestimate the mobility of the ends. It should be pointed out here that at infinite time in the absence of excluded volume, the bead distribution profile will be parabolic, *independent of the particular model of the dynamics.*

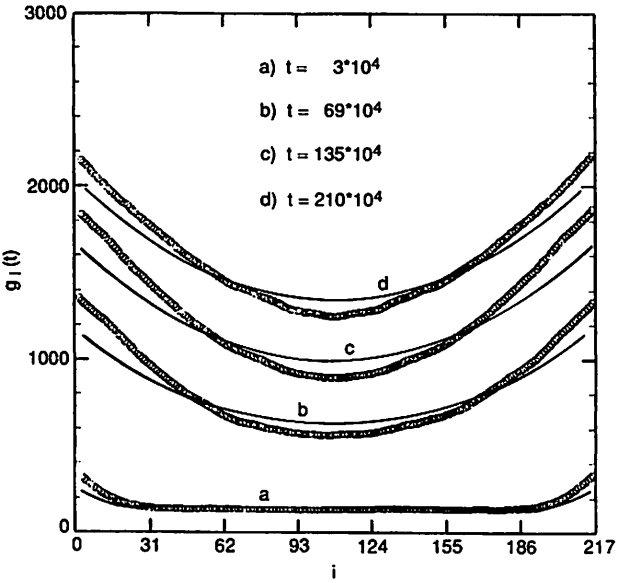

Figure 12. Time dependence of the mean-square displacement of the ith bead as a function of position along the chain for $n = 216$ linear chains confined to a diamond lattice at $\phi = 0.5$.

2. *Nature of the Contacts between Chains*

To examine the time evolution of the contacts between chains, the following algorithm is employed.[16] (1) Each chain is replaced by a series of nonoverlapping blobs, each having n_b monomers. (2) All pairs of blobs belonging to different chains, whose centers of mass lie a distance less than $r_{\min} = 5$, are identified. (The length of a bond equals unity.) (3) The number of such contacts is counted. (4) The fraction of contacts, $n_c(t)$, that survive up to a time t later, given that the blobs were in contact at zero time, is determined.

For the $n = 216$, $\phi = 0.5$ cubic lattice chains, $n_c(t)$ is found to be decomposable into a sum of three exponentials.[16] While this decomposition is of course not unique, the results are highly suggestive. The majority of the contacts (64%) decay within 1% of τ_R, 91% decay within 9% of τ_R, and the remaining contacts decay on the order of τ_R. This translates into one long-lived contact every 133 beads. If Eq. (15a) is used to extract the number of monomers between entanglements, one finds a value of 125. The mean lifetime of these contacts is consistent with the idea that long-lived contacts between polymers slow down the motion of the chains at long times. Most local contacts are short lived, and apart from modifying the local monomeric friction constants, they exert no effect on the long-time dynamics.

The first conclusion that emerges from the simulation is that long-lived dynamic entanglement contacts occur on a distance scale which is an order of magnitude larger than the static excluded volume screening length. In real polymer melts, the excluded volume screening length is on the order of a monomer unit;[25] whereas, based on estimates from the plateau modulus and the crossover regime of the shear viscosity, the mean number of monomers between entanglements is on the order of 100 monomers or so.[3,26] Moreover, by examining the displacement of the contacts, we have established that all entanglements are moving with respect to the laboratory fixed frame and that there is no static cage. If these model chains were reptating, in a fixed tube no single contact should live on the order of the terminal relaxation time.

What then might dynamic entanglements be? Suppose that at zero time a pair of chains are in a configuration where one chain loops around another chain. This may be a necessary, but not sufficient, condition for the formation of an entanglement. Subsequently, the pair of chains must move in a direction that causes the entanglement to be long lived; that is, one chain drags another chain for times on the order of the terminal relaxation time. Whether or not the disengagement must occur by reptation is not yet established, nor is it clear what sort of configurations cause the dynamic entanglements. The analysis of these kinds of questions is now underway; however, at best, the results must be viewed as tentative. Even in the $n = 800$ linear chains, there are at most 6–7 entanglements per pair of chains, and their statistics are likely to be poor.

E. Cooperative Relaxation Dynamics

In a series of papers Pakula and Geyler,[69–71] have developed a method of simulating chains on a fully packed lattice, using a cooperative exchange mechanism that works as follows. (1) A kink on a given chain is chosen, say chain A. This kink is sliced out of the chain and inserted into a section of chain B that is locally parallel to the top section of the original kink in chain A. Observe that this decreases the length of chain A, and temporarily increases the length of chain B. (2). The algorithm then searches for a similar interchange between chain B and another chain C. (3) The loop replacement procedure is continued until a loop is interchanged back with the original chain A. Thus, at the end of a loop migration procedure, all the chains have been restored to their original contour length. While there is no doubt that this is a highly efficient algorithm for equilibrium sampling, it is not clear how reliable the resulting dynamics are, especially since there is no limitation on the lengths of the mobile loops. They choose 10^6 searching steps as the fundamental time unit; this particular choice, at short time intervals, produces equal mean square displacements of the monomers that are independent of chain length. A possible problem encountered if this algorithm is employed

to obtain dynamic sampling is that in a single time unit, interchanges over short and long wavelength distance scales are occurring, and it is not at all clear how (or even if) the time scale is distorted.

Applying this cooperative motion model to a melt of linear chains confined to a cubic lattice, chains up to $n = 512$ were simulated.[70] For longer chains, the self-diffusion coefficient is found to have a $D \sim n^{-2}$ regime, and the end-to-end vector autocorrelation functions are found fit a stretched exponential form. The single-bead autocorrelation function is found to be close to that predicted by the Rouse model. Snapshots of individual chain configurations indicate globally isotropic dynamics with no evidence of reptation.

They next applied their algorithm to examine the dynamics of a melt of rings;[71] the equilibrium results have been summarized in Section II.C.2. They find that rings have a *smaller* self-diffusion constant than the corresponding linear chains, and while this difference decreases with increasing n, it disagrees with the viscoelastic experiments which indicate that melts of rings are more mobile than the corresponding linear chains. The origin of the difference between their results and the local MCD simulations of Section II.C.2 is not clear. One thing the linear simulations point out, however, is that a D proportional to n^{-2} appears to be a ubiquitous result that cannot be invoked as proof of chain reptation. This point is addressed further in Section III.B.1.

F. Dynamics of Chains in Random Media

To examine the fundamental validity of the reptation model Muthukumar and Baumgartner[50,51] have returned to the original system on which the reptation idea is based and have performed off lattice, MC simulations on a single chain diffusing through a random medium. The mean-square displacement of the center of mass of the chain is observed to exhibit three time regimes. At long and short times $g_{cm}(t)$ is linear in time. The duration of the intermediate time regime increases as either the chain length or the volume fraction of the solid phase increases. The short-time apparent diffusion constants are Rouse-like with $D_{app} \sim n^{-1}$. The diffusion constants extracted from the long-time behavior of $g_{cm}(t)$ do not obey the n^{-2} scaling predicted on the basis of the reptation model. Rather, the results indicate the presence of entropic barriers, arising from the necessity of the chain squeezing from one domain to the other through bottlenecks. Thus, even in the case of a static random medium, it does not automatically follow that a chain must reptate. While it is true that as the contour length of the chain increases to the point that a given chain may be in multiple domains, then reptation-like motion will dominate, it is not necessarily true that classical reptation theory should apply. The latter situation appears to hold in the problem of DNA gel electrophoresis and has been analyzed by Levene and Zimm.[75] A further discussion of the theoretical problems associated with DNA gel electro-

phoresis is beyond the scope of this article. For additional details, we refer to the literature.[75-77]

G. Brownian Dynamics Simulation of Polymer Melts

Kremer, Grest, and co-workers[24,78] have undertaken a series of Brownian dynamics simulations of an off-lattice model of a polymer melt. We remind the reader that in Brownian dynamics one solves Newton's equation of motion for the system coupled to a heat bath. In their particular realization, the inertial term is retained, while in many simulations since polymers are typically in the high friction limit, it is dropped.[79] They have studied the dynamics of up to $n = 400$ chains confined to a box containing $N = 10$ polymers. Their results can be summarized as follows. They find for $n > 35$, a crossover to $D \sim n^{-2}$, scaling. For $n < 35$, $Dn \sim$ constant is seen, and $g_5(t)$ is Rouselike. As n increases further just as in the cubic lattice system, there is a crossover to $t^{1/4}$ behavior, which these authors interpret as due to reptation. Further analysis of the primitive path dynamics indicates that for the range of times sampled, the reptation component of the motion is important. These authors again interpret this as proving the existence of reptation. Unfortunately, they only sample the dynamics, at best, to the end of the $t^{1/4}$ regime, and as we have discussed in Section II.A.2, it is not until the end of this regime that the lateral component of the motion begins to dominate to the point that reptation can be neglected. Moreover, neither the existence of a $t^{1/4}$ regime nor the scaling of D, as the inverse square power of n, is unique to reptation. Thus the Kremer et al.[24,78] simulations agree with the MCD simulations of Kolinski et al.[23,47,48] in the time regime that they overlap, and the Kremer et al. case for reptation is not at all definitive.

III. THEORETICAL TREATMENTS OF POLYMER DYNAMICS

There have been a number of theoretical models developed over the years to describe the dynamics of entangled polymers. Briefly, these can be divided into three general categories. First of all, there is the classical reptation theory in which there is always a well-defined tube constraining the chain of interest.[1,4-9,13,37] This tube exists for times on the order of the terminal relaxation time of the end-to-end vector. Hence, the dominant long-wavelength motion involves the slithering down of the contour for times on the order of the terminal relaxation time. This model has a very large number of variants and is by far the most highly developed. As these models have been extensively discussed in detail elsewhere,[1] we refer the reader to the literature for a detailed exposition of their properties.

The second class of models envisions the polymer environment to be more liquid-like. Entanglements between chains are still important, but they are

dynamic in nature. The models of Fujita and Einaga,[9,10] Skolnick et al.,[16,17] Ngai et al.,[14,74] and Fixman,[18,19] fall into this category. The qualitative description of each of these models is presented in turn below. Finally, there is the hydrodynamic interaction model of Phillies,[11,12] in which entanglements in concentrated polymer solutions are relegated to a minor role and interchain hydrodynamic interactions are assumed to dominate. While the theory has been developed to treat the case of concentrated solutions, since it is clearly related to the problem of dynamics in a melt, an overview of this alternative view is clearly appropriate. As will become apparent, there are a number of quite different viewpoints of the nature of polymer melt dynamics, and this, no doubt, reflects the intrinsic difficulty of the problem.

A. Fujita–Einaga Theory—The Noodle Effect

For the case of concentrated polymer solutions and polymer melts, Fujita and Einaga[9,10] argue that dense polymer systems do not suffer from the severe topological constraints conjectured by reptation theory; rather, in entangled systems, moving chains induce the movement of surrounding chains through the interactions at entanglement points, thereby producing considerable energy dissipation. These authors refer to the cooperative motion of the surrounding chains as the "noodle effect."

1. Diffusion Constant

These authors[9] then proceed to calculate the diffusion coefficient of a chain in the case of a monodisperse system in the $n/n_e \gg 1$ limit, where n_e is the mean number of monomers between adjacent entanglement points. Assuming that the translational friction coefficient of a chain can be expressed as the product of n times a mean monomeric friction coefficient ζ by the standard Stokes–Einstein relationship, the polymeric diffusion coefficient is

$$D = k_B T/(n\zeta), \tag{18}$$

with k_B Boltzmann's constant and T the absolute temperature. If the entangled segments are assumed to be localized at every n_e bead, each of which has an additional friction constant ζ_e in addition to the friction constant in the absence of entanglements ζ_0, then in the large n/n_e limit the average monomeric friction constant is

$$\zeta = \zeta_0 + \zeta_e/n_e. \tag{19}$$

Thus the crux of the model involves the calculation of ζ_e.

Fujita and Einaga make two assumptions from which ζ_e follows. First, they assume that the velocity field E, induced around the test chain when the test

chain moves with velocity u, is spherically symmetric about the center of mass G, and its radius is of order $\langle S^2 \rangle^{1/2}$, the root mean square radius of gyration. In particular, they take the radius of E to equal $2\langle S^2 \rangle^{1/2}$, which is proportional to $n^{1/2}$. Second, they invoke the free drainage approximation (i.e., they neglect hydrodynamic interactions between segments) and proceed to calculate the force F in the direction u that must be applied to G to overcome the frictional force exerted by all the chains on the test chain

$$F = \zeta_0 \int_E \rho_e \bar{u}\, dv. \tag{20}$$

Here, ρ_e is the average segment density in the volume element dv which moves cooperatively with the test chain, and $\bar{u}$ is the average velocity of the coupled segments in the u direction. It is quite reasonable that ρ_e and $\bar{u}$ monotonically decrease as one goes out from the center of mass.

They replace $\bar{u}$ by ku with k a constant between zero and one that is taken to be independent of n, polymer concentration, and position within the velocity field E. In this approximation, Eq. (20) becomes

$$F = \zeta_0 ku \int_E \rho_e\, dv. \tag{21}$$

They then approximate by $N_c s$, where N_c is the number of chains directly entangling with the test chain and s is the number of segments of such an entangling chain that has substantial coupling with the test chain and which are located inside the field E.

Now the spherical domain occupied by each of the entangling chains has $(n/n_e)^{1.5} n_e$ entangling segments [there are $(n/n_e)^{1.5}$ entangling units in the volume $2\langle S^2 \rangle^{1/2}$, each contains n_e segments]. The essential assumption is then made that s is proportional to $(n/n_e)^{1.5} n_e$, with a proportionality constant that is independent of the polymer concentration. This assumption assumes that a fraction of the chains not involved in direct entanglements with the test chain are also dragged along with it.

Employing these assumptions, Eqs. (18–21) give

$$\zeta_e = \zeta_0 f n^{3/2} n_e^{-1/2} \tag{22}$$

with f a constant. Thus the effective monomeric friction coefficient is

$$\zeta = \zeta_0 [1 + f(n/n_e)^{3/2}]. \tag{23a}$$

When ζ is inserted in Eq. (18), the self-diffusion coefficient is

$$D^{-1} = n\zeta_0(k_BT)^{-1}[1 + f(n/n_e)^{3/2}]. \tag{23b}$$

Equation (23b), therefore predicts that D asymptotically should be proportional to $n^{-5/2}$, a behavior not inconsistent with experiment.[9,80]

One of the touchstones of a successful theory is the ability to rationalize not only the molecular weight dependence of a monodisperse polymer melt, but also to rationalize the independence of the probe diffusion coefficient on matrix molecular weight when the latter is sufficiently large. In their treatment Fujita and Einaga[9] consider a bidisperse blend of polymers having degree of polymerization n_1 and n_2 for components 1 and 2. Both components are assumed to be sufficiently long that they exhibit entangled behavior and $n_2 < n_1$. The key to this analysis lies in the assumptions indicated above that only chains within several (two) radii of gyration of the chain of interest are dragged along with the probe chain. This leads to the prediction that the increase in friction coefficient is identical to Eq. (22), with n_2 substituted for n, and where n_e is given by the reciprocal average of the mean number of monomers between entanglements arising from chains 1 and 2. Thus the desired independence of matrix molecular weight is recovered with $D_p \sim n_2^{-5/2}$. However, fits to experiment did not reveal the theoretically predicted power of D_p.

Einaga and Fujita[9] have also been able to derive a prediction of the concentration dependence of D, which obtains from the recognition that n_e should be inversely proportional to polymer concentration c_p. This simply gives $D \sim c_p^{-1.5}$. Experimental data give varying power law (or perhaps not; see the Phillies theory,[11,12,34] Section III.D) dependencies of D, ranging from the -3 to -1.75 power. However, different c_p scaling can be obtained depending on the molecular-weight dependence assumed.

2. *Viscosity*

Fujita and Einaga[10] have also developed an expression for the steady-state shear viscosity of a polymer blend, η_0. They basically employ standard linear viscoelasticity theory plus the assumption that the terminal relaxation time of each component τ_{mi} is given by

$$\tau_{mi} = Bn_i/D_i, \tag{24}$$

where B is a constant and D_i is the diffusion coefficient of the ith component of degree of polymerization n_i. In the case of a monodisperse system, it then follows that η_0 is predicted to be proportional to the 3.5 power of the molecular weight. By assuming that the shorter chains relax as if they were in a noninteracting blend, they also derive an expression for η_0 appropriate to this situation.

The key point is that this theory predicts for a monodisperse system that $D\eta_0 \sim n$. Furthermore, this analysis shows how an alternative mechanism to reptation based on the assumption that what is relevant is the dragging of chains for distances on the order of the radius of gyration, can give rise to a plausible physical picture that overall is in fairly good agreement with experiment. It is interesting to note that reasonable scaling behavior can be predicted without, in fact, specifying whether the chains ultimately disengage by reptation, or perhaps by some other mechanism.

B. Phemonenological Theory of Dynamic Entanglements

1. *Diffusion Constant*

Based on the discussion above, the question arises as to just how general the treatment must be to recover the experimentally observed scaling of D and η with n. The following development by Skolnick et al.[16,17] is patterned after the Hess[13,81] generalized Rouse treatment, which was used to provide a theoretical underpinning for reptation-like behavior. The key to Hess' recovery of reptation is the assertion that the forces exerted on the test chain by the sea of surrounding chains act perpendicular to the chain axis. Since the Kolinski et al.[23,47,48] simulations indicated that this is only true for a small fraction of time in the intermediate time regime, we modified the treatment to account for the observed isotropic motion of the chains. In particular, because the behavior of the chains is Rouse-like, the motion is factored into two components, the center of mass motion between the chains and the motion of the internal Rouse-like coordinates, with a weak coupling between the two permitted.

Starting from the Green–Kubo expression for the diffusion constant, Hess employed Zwanzig–Mori projection operator techniques to obtain the enhanced friction constant acting on the test chain due to the other chains.[13] After a bit of arithmetic,

$$D = \frac{k_B T}{n[\zeta_0 + \int_0^\infty dt \Delta\zeta(t)]}. \tag{25}$$

Here ζ_0 is a generalized concentration-dependent Rouse monomer friction coefficient, and $\Delta\zeta$ is the additional dynamic friction term arising from interchain interactions. If a standard separation of time scales argument is made, the effects of short-lived contacts can be subsumed into an effective molecular weight independent, monomeric friction coefficient ζ_0. The effect of the long-lived, but dilute dynamic entanglements between chains are reflected in $\Delta\zeta$, which is explicitly defined as

$$\Delta\zeta(t) = \frac{\langle F(t)\cdot F(0)\rangle}{3nk_BT} \tag{26}$$

where the term in the brackets is a Zwanzig–Mori projected force correlation function.

In order to evaluate $\Delta\zeta$, the following assumptions are made. First, interactions between chains are assumed to be predominantly steric in nature and hydrodynamic interactions are ignored. Second, the time evolution of $\Delta\zeta$ reflects the motion of the dynamic entanglements. Finally, because dynamic entanglements are dilute, the interaction hierarchy can be truncated at the pair level. Using these assumptions, it is straightforward to show that the propagator for pairs of chains in contact in the long-wavelength, hydrodynamic limit is of the form

$$R(q,t) = \exp(-D_{\text{eff}}q^2t) \tag{27}$$

where D_{eff} is an effective diffusion constant and q is the magnitude of the wave vector.

A plausible functional form for D_{eff} is given by

$$D_{\text{eff}} = (1-\beta)D_0 + \beta D. \tag{28}$$

D_0 is the renormalized Rouse diffusion coefficient given by

$$D_0 = k_BT/n\zeta_0 = d_0/n. \tag{29}$$

Equation (28) accommodates the fact that for times of order of the terminal relaxation time the behavior is essentially Rouse-like (see Sections II.A and II.D.1), but with a small coupling between the center of mass motion and the internal coordinates. In the small coupling limit ($\beta \ll 1$), it follows that

$$D = \frac{d_0}{n(1+n/n_e)}. \tag{30}$$

Here n_e is the average number of monomers between dynamic entanglements.

An analogous equation can be derived for the diffusion coefficient of a probe in a matrix, which in the small coupling limit gives

$$D_p = \frac{d_0}{n_p}\left[\frac{1+n_p/n_m}{1+n_p/n_m+2n_p/n_e}\right] \tag{31}$$

where n_p (n_m) is the degree of polymerization of the probe (matrix) chains.

Equation (30) and (31) provide rather good fits to simulation results described in Sections II.A–II.C as well as to the experimental data of Antonietti et al.[67] on polystyrene melts and predict that D_p should scale asymptotically as n_p^{-2}. A more detailed description of the model that describes the behavior of the self-diffusion constants over the entire range of β is given elsewhere.[16,49]

Since the assumptions employed to derive Eqs. (30) and (31) are so benign, the existence of an n^{-2} power law dependence of D cannot be used to prove the existence of any particular microscopic model of chain motion. It differs from the Fujita–Einaga result[9] in that the latter assumes stronger coupling between entangled chains, and here a weak coupling limit is assumed.

2. *Viscosity*

We next review those features that any successful theory must rationalize about the internal dynamics of polymer melts. It must reproduce the molecular weight dependence of the diffusion coefficient and the viscosity.[1,26–33,35,67] It must also be consistent with the simulation results[23,47,48] that indicate that the chain motion is slowed down and in many ways Rouse-like and that there is no tube confining the chains. The single bead autocorrelation function has a t^b regime with $b < 1/2$, and g_{cm} has a t^a regime with $a < 1$. The product $D\tau_R/n$ scales as n^ε with ε, assuming values between 0.1 and 0.2. Finally, it must rationalize the single-bead mean square displacement profiles which indicate that the ends are more mobile than the equivalent Rouse chain and the middle is less mobile (see Fig. 12).

We summarize below the features of a recent phenomenological theory that accounts for the above features. The following simplifying assumptions are made. (i) At short times, a la Doi and Edwards,[5] the response of the melt is treated as rubber. We then focus on the motion of an average reporter chain and assume that the long-time relaxation behavior in a polymer melt is adequately described by a Rouse model; however, because of the presence of dynamic entanglements there are n/n_e slow moving points, each of which drags another chain along with it. In the effective single-particle picture, these slow moving points have an augmented monomer friction constant of order n. This approximation assumes that for times on the order of the terminal relaxation time, on average the matrix chains are dragged along with the test chain and the dissolution of the contact can be ignored. This clearly is the simplest approximation of the effect of entanglements. It neglects the coupling between the various entanglements and the time course of their dissolution and formation.

With these assumptions in hand, the following qualitative picture of the dynamics emerges for the expected crossover behavior of the individual chains. Suppose an individual chain has just one entanglement. Physically, one would expect this entanglement to be located at or near the center of the chain.

Clearly, this one slow-moving point wouldn't change the behavior of the terminal relaxation time of the end-to-end vector by much; the single slow-moving point behaves like a local defect. However, in the absence of the entanglement, the self-diffusion coefficient is d_0/n, and in the presence of the entanglement, it is $d_0/2n$. In other words, the crossover behavior of D and τ_R should be different, in agreement with experiment. Moreover, the center of

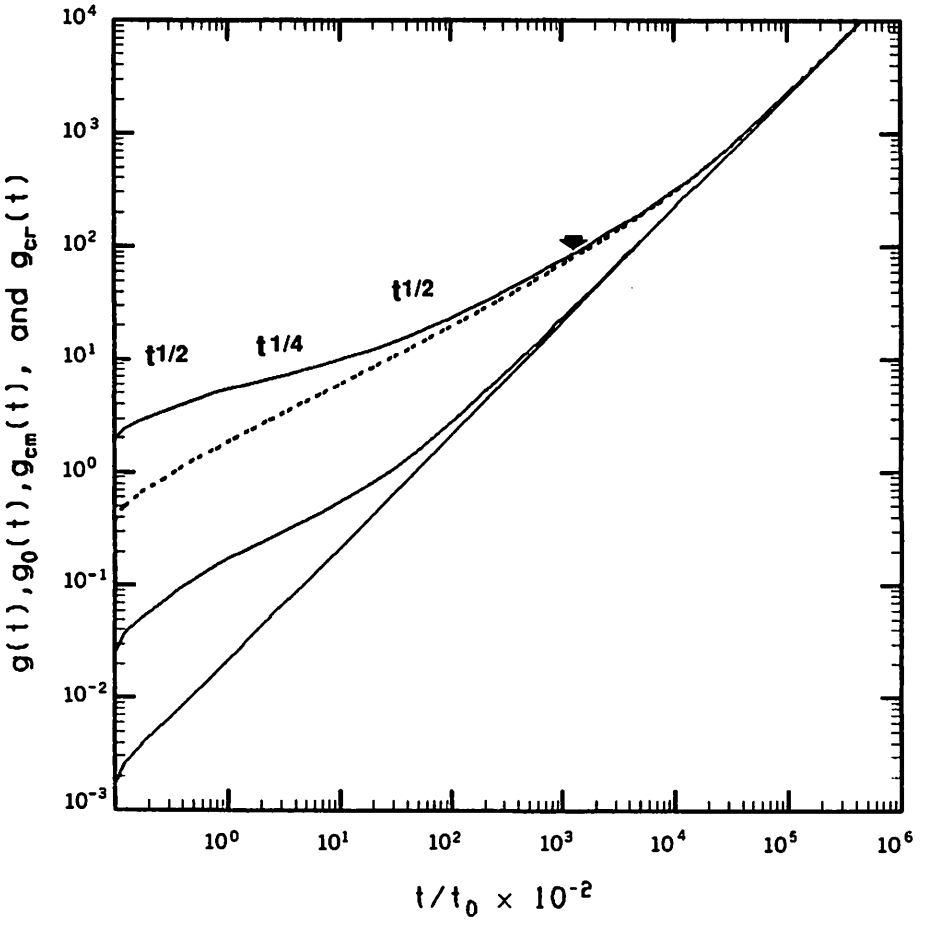

Figure 13. In the curves going from top to bottom, log–log plots of $g(t)$, the mean square displacement per bead obtained assuming that each bead has a uniform friction constant $g_0(t)$, the mean square displacement of the center of mass $g_{cm}(t)$, and the mean square displacement of the center of frictional resistance $g_{cr}(t)$; t_0 is the average time a monomer takes to diffuse a bond length. See text for further details.

mass and the center of frictional resistance are no longer the same.[42] Basically, the center of mass motion couples into the internal coordinates, and this gives rise to the $g_{cm}(t) \sim t^a$, for values less than $2\langle S^2 \rangle$. Similarly, a t^b regime is predicted for $g(t)$.

It is also possible to show that in the limit as n goes to infinity, the dynamic properties behave as if each monomer has an effective friction constant $\zeta_0(1 + n/n_e)$ with ζ_0, the monomeric friction coefficient in the absence of chain connectivity. The viscosity equals 4/15 of the Doi–Edwards[37] value, and ultimately scales as n^3. Thus, in the crossover regime, the viscosity scales as $n^{1+\delta}$ with δ going to zero, as n goes to infinity. Finally, the product of the plateau modulus times the shear compliance equals 10/7, while Doi–Edwards theory gives a value of 6/5, and experiments give values in the range of 2.5 to 3.[37]

Fits to a number of assumed distributions of slow-moving points give $\eta \sim n^{3.4}$, with a lower bound for the crossover value of $\eta \sim n^3$, around 40–50 entanglements. This is not inconsistent with the recent work of Colby et al.,[35] but the experiments themselves are the subject of controversy.

The present theory predicts that the crossover value of n_c', is about $4.5n_c$. Thus, in accord with the experiment[35] (see Eqs. 1 and 2), the viscosity exhibits the 3.4 power of the molecular weight, prior to the crossover of the diffusion constant into the n^{-2} regime. Finally $D\,\tau_R/n$ has an n^ε regime with $\varepsilon = 0.1$ or 0.2, depending on the particular distribution of friction constants.

Finally, in Fig. 13 log–log plots of $g_{cm}(t)$ and $g(t)$ versus time are presented for the case of an $n = 255$ chain with a mean distance between entanglements of 15 and a τ_R of 1.88×10^5. This τ_R value of the corresponding Rouse chain is 1.3×10^4. In the top solid curve, there are $t^{1/2}$, $t^{1/4}$, and $t^{1/2}$ regimes in $g(t)$, and these chains are clearly not reptating. This is but another example that shows that the existence of a $t^{1/4}$ regime in $g(t)$ is indicative of some kind of constrained dynamics, but it need not be reptation.

C. Coupling Model of Polymer Dynamics

Over the past decade Ngai, Rendell, and co-workers, have developed a general formalism to address the problem of how[14,74,82] the relaxation of a "primitive" mode is modified by the coupling to complex surroundings. The fundamental prediction of the model is that the net effects of such coupling can be accounted for by the use of a time-dependent relaxation rate. As will be seen below, their application to polymer dynamics is in the same philosophical spirit as that of the two previous models, but affords the advantage that it explicitly accounts for the time-dependent modification of the behavior of the chain.

The coupling model asserts that the coupling of the primitive relaxation mechanism to the environment slows down the primitive relaxation rate W_0 for times greater than a characteristic time $t_c = \omega_c^{-1}$. In other words, there is

a time-dependent relaxation rate $W(t)$ of the form

$$W(t) = W_0 \qquad \omega_c t < 1, \tag{32}$$

$$W(t) = W_0(\omega_c t)^{-n} \qquad \omega_c t > 1.$$

The relaxation function $c(t)$ then obeys the rate equation

$$\frac{dc}{dt} = -W(t)c, \tag{33}$$

and the normalized relaxation function $\phi(t) = c(t)/c(0)$ is of the form

$$\Phi(t) = \exp(-t/\tau^*)^{1-n}, \tag{34}$$

and the terminal relaxation time is

$$\tau^* = [(1-n)\omega_c^n \tau_0]^{1/(1-n)}. \tag{35}$$

The degree of coupling is embodied in the parameter n (not to be confused with the degree of polymerization; we employ the Ngai et al.[14,74,82] notation to facilitate comparison with the original papers). For chain molecules in the melt, τ_0 is the terminal relaxation time of the nonentangled Rouse chain. The particular value of n is taken to depend on the particular kind of experimental measurement. For the case of shear viscoelasticity, they report the following predictions. The terminal dispersion of the shear modulus is of the Kohlraush, et al. form,[83] and the terminal relaxation time can be calculated from τ_0 using Eq. (35) for $\Phi(t)$. The former prediction is in accord with a number of experiments.[14] Thus, using Eq. (35) and the Rouse τ_0, τ_η^* can be extracted. These fits provide a values of n_η in the range of 0.4 to 0.45. If one then approximates the viscosity by the relation $G_N^0\tau^*$ with G_N^0, the plateau modulus, then

$$\tau^* \sim M^{2/(1-n_\eta)}[\zeta_0(T)]^{1/(1-n_\eta)}. \tag{36}$$

In Eq. (36), M is the molecular weight of the polymer. Using the values of n_η obtained from the experiment gives a molecular weight dependence of the viscosity between 3.3, and 3.6, in good agreement with experiment. Equation (36) also provides an estimate of the temperature dependence of τ_η^* that is in agreement with experimental measurements on polyethylene and hydrogenated polybutadiene. Finally Eq. (36) provides a relationship between the viscosity activation energy E_η^* and the monomeric friction constant activation energy E_a,

$$E_\eta^* = E_a/(1 - n_\eta), \tag{37}$$

a relationship also found to agree with the experiment.[14]

They[84] have also deduced the molecular weight dependence of the diffusion constant. They proceed by relating the observed activation energy of the diffusion constant E_D^* to the monomeric diffusion constant by the analogous relation, as in Eq. (37). This provides a value of n_D of 0.33, and a characteristic relaxation time associated with diffusion of $\tau_D^* = M^{2/(1-n_D)}$ which scales as M^3. By assuming that $D \sim \langle S^2 \rangle / \tau^*$, they recover the inverse squared power dependence of D on M.

More recently, Ngai et al.[85,86] have also derived a relationship for the molecular weight dependence of a probe chain dissolved in a matrix that is in good agreement with experiment for both linear and star tracer molecules. Furthermore, they have obtained the stretched exponential form for the concentration dependence of D (see Eq. 2). They identify the origin of the stretched exponential with the gradual increase of the coupling between a diffusant and the matrix as the concentration of the diffusant increases; that is, the coupling parameter $n(c)$, monotonically increases with increasing concentration c.

In a recent publication Ngai and Lodge[86] applied the coupling model to treat the diffusion of 3- and 12-arm polystyrene stars in entangled PVME solutions. They find excellent agreement with experiment. Moreover, their treatment predicts a different temperature dependence for stars than the corresponding linear chains, a prediction that is also in accord with experiment. Thus, in application to extant experimental data, the coupling model is in rather good agreement with experiment, without invoking the existence of reptation. The qualitative picture is also in accord with simulation data[18,23,47,48,69–71] that does not provide support for the existence of reptation within a spatially fixed tube. The only problem with the theory is that it cannot, as yet, predict the values of the coupling parameters, nor does it identify the particular mechanism responsible for the coupling. Nevertheless, in spite of these limitations, the coupling model is a very powerful approach that appears to have much to say about the dynamics of entangled polymer systems.

D. The Fixman Model of Polymer Melt Dynamics

In a recent pair of papers, Fixman[18,19] has proposed a generalization of the reptation model of polymer dynamics that has as its basis the following assumptions. First, it assumes that the most naive view of both simulations and experiments are correct. That is, the viscosity $\eta \sim n^{3.4 \pm 0.1}$ is indeed the asymptotic power law, that the highly cooperative and simultaneous motion of the chains, seen in simulations,[17,23,47,48,61] is correct at all chain lengths

(i.e., there is no frozen matrix) and, finally, that the translational friction coefficient for self diffusion scales as n^2. As will be seen below, unlike the treatments discussed above that in many respects are highly phemonenological, Fixman has attempted to identify the specific mechanisms responsible for entangled melt behavior and proposes a formalism for calculating the polymeric properties arising from this conjectured behavior.

Taking these assumptions as valid implies that chains can diffuse many radii of gyration without orientational relaxation.[35] The persistence of entanglements during the process of diffusion across many radii of gyration is rationalized in terms of the correlated reptative motion of the probe and vicinal (matrix) chains. The mathematical formalism is cast in terms of generalized Langevin equations for the motion of the probe and has as its basis the Rouse–Zimm model of chain dynamics at infinite dilution. In particular, Fixman assumes that the matrix surrounding the probe chain is capable of exerting a viscoelastic response to any forces exerted on it. But unlike the isolated chain case where the elastic part is essentially neglected, in the case of melts, the elastic part is assumed to be important. In addition to the viscoelastic response, the matrix chains are themselves capable of reptative motion along their respective primitive paths. Fixman asserts that for the consistency of the treatment of viscoelastic interactions, the reptative motion of the probe chain is accompanied by reptative motion of the matrix chains; that is, unlike in standard reptation theory, here the motion of the probe and matrix chains is taken to be highly correlated. Entanglements are identified as small loops or twists of one chain about the other.

Imagine then the response of the polymeric system to an external force. Owing to the elastic deformation of the matrix, the displacement of the probe chain with respect to the laboratory fixed frame increases, concomitantly, the reptative diffusion relative to the deforming matrix slows down. The net result on the translational diffusion of the probe of these two opposing effects is predicted to be negligible, if both the probe and vicinal chains are of the same length. However, unlike standard reptation theory, the friction constant for reptative motion increases by a factor $n^{1-x_s} \cdot x_s$ assumes the value of one-half, if Gaussian statistics obtains and 0.6 if excluded volume statistics applies. Furthermore, the translational diffusion constant $\sim n^{-2}$, and the viscosity scales like n^{4-x_s}.

In a companion paper[19] Fixman applied his formalism to calculate the storage and loss modulus, the shear compliance, and the translational diffusion coefficient using parameters appropriate to polybutadiene. The resulting dynamic stress modulii are in fairly good agreement with experimental results. A particularly important conclusion is that the Langevin equation has the same normal mode structure as in Rouse–Zimm[42] theory, but each mode relaxes as a sum of exponentials, rather than just a single exponential (perhaps

providing the underpinnings for the Ngai et al.[14,74,82,84–86] coupled model, KWW functional form). Fixman points out that there his approach requires a number of not-well-determined parameters; nevertheless, the theory is rather impressive in its agreement with experiment.

At this junction it is appropriate to summarize the various viewpoints. In all the theories discussed above, there is the implicit assumption of the cooperative relaxation of the test chain with its surrounding matrix of chains. That is, the motion of the probe and matrix chains are coupled, and there is no fixed matrix confining the chain of interest. Furthermore, the entanglements are envisioned to be of a dynamic nature, and not static as in the classical reptation model. In fact, the various theories differ in their specification of what mechanism, if any, is responsible for entanglement disengagement. In all but the Fixman theory, the disengagement mechanism is left unspecified. Fixman asserts that the dominant long-time disengagement mechanism is by reptation. Furthermore, all the other theories implicitly or explicitly assume that the decay distance for orientational correlation is on the order of the radius of gyration of a chain, whereas Fixman envisions this as occurring over many radii of gyration. What is clear, however, from the discussion of all the aforementioned theories is that (more or less) they all reproduce most, if not all, features of experiment, and more sophisticated tests will have to be devised to determine which, if any, are in fact correct.

E. Hydrodynamic Interaction Theory of Concentrated Solutions—The Phillies Model

For the case of concentrated polymer solutions, Phillies[34] has found that the stretched exponential form for the self-diffusion coefficient,

$$D = D_0 \exp(-\alpha c^{\nu}), \tag{38}$$

fits the entire concentration range for all extant studies of the concentration dependence of D. In fact, the stretched exponential form fits the concentration dependence of both high- and low-molecular-weight polymers, as well as for globular, nonentangling proteins. Since globular proteins cannot entangle (they are rigid, dense bodies), Phillies[34] argues that the same physics underlying the motion of dynamics of globular proteins should hold for polymer solutions as well. Unlike the Ngai and Lodge treatment described above[86] (see Section III.C). Phillies has developed a model that gives the functional form of Eq. (38), and numerical values of α and ν.[11,12] Thus, more than one physical picture can reproduce Eq. (38), and in fact Adler and Freed[87] have derived Eq. (38) in the context of a mean field approximation. The Phillies approach is especially useful in that it provides for quantitative values for all of the parameters.

The fundamental assumptions of the Phillies model[11] are: (1) There is a self-similar effect of infinitesimal concentration increments on D. (2) The dominant force between polymers in semidilute solution is hydrodynamic. (3) The root mean square radius of gyration is described by the blob model of Daoud et al.[88] that is, $\langle S^2 \rangle \sim Mc^x$ with $x = -1/4$. An overview of his derivation of Eq. (38) follows.

From assumption (1), the increase in the mobility μ arising from a concentration increment Δc is taken to be

$$\mu(c + \Delta c) = \mu(c) + A\Delta c, \tag{39}$$

where A is assumed to be proportional to $\mu(\Delta c)$. The dependence of A on polymer dimensions is taken from hydrodynamics by employing the functional form appropriate to interactions between hard spherical particles, namely, $A \sim \langle S^2 \rangle^{1/2}_a \langle S^2 \rangle^{3/2}_b$, and where a refers to the test polymer and b refers to the other chains in solution.

The key to the argument comes next, where assumption (3) is invoked; namely,

$$\frac{d\mu}{\mu} = a(c)\,dc, \tag{40}$$

with $a(c) = A/\mu$. By examining the functional form for μ, as a function of c, Phillies replaces A/μ by A/μ_0, with μ_0 the mobility at infinite dilution. Integrating Eq. (40) and using the Stokes–Einstein relation between D and μ gives

$$D(c) = D_0 \exp\left(\int_0^c \frac{A(c)}{\mu_0} dc \right). \tag{41}$$

If the scaling of $\langle S^2 \rangle$ of the probe and matrix with concentration is used, one finds that

$$\int dc \frac{A(c)}{\mu_0} = \alpha c^v \tag{42}$$

where $\alpha \sim M$ and $v = 1 - 2x$. An analogous development of Eqs. (40) and (41) has been previously presented by Adler and Freed.[87]

In subsequent work, in the spirit of the hydrodynamic interaction model of concentrated polymer solutions, Phillies[12] derived an explicit functional form for $A(c)$. The specific approach is based on a generalization of Einstein's derivation of the Stokes–Einstein diffusion equation. In particular, the method of reflections is used where a series of velocities are calculated. The first

polymer is assumed to have an unperturbed mobility. This then acts on the second polymer, which creates a velocity echo that perturbs the original polymer's flow field and consequently its mobility. The treatment, in detail, involves the generalization of the Kirkwood Riseman[89] model from one to two polymers. The net result is that

$$\alpha = -\frac{9}{16}\frac{\langle S^2\rangle_a^{1/2}}{2a_0}\frac{4\pi}{3}\frac{\langle S^2\rangle_b^{3/2}}{M_b}\frac{1}{1-2x}, \tag{43}$$

where a_0 is the radius of a monomer. Note that Eq. (43) predicts that $\alpha \sim (M_a M_b)^{1/2}$ in agreement with previous scaling arguments.[11]

For the case of polystyrene at $M = 1 \times 10^6$, Phillies estimates α is about -2. Fits to experiment give an α of -0.7. However, over the entire range of α, Phillies reports rather good agreement with the experiment, with α ranging over more than 3 orders of magnitude as M changes.

Phillies further argues that α should be similar for both linear and star molecules, which appears to be in agreement with experiment.[12] In a recent pair of papers,[90,91] however, Lodge et al. find that D_0 values fit to linear polystyrene data are systematically greater than the measured values and that the expected scaling of α with molecular weight is not found, in contrast to previous results.[34] For the case of stars, Eq. (38) reproduces the concentration dependence very well, but the origin of the chain architecture dependence is unclear. Thus, a controversy between the Lodge and Phillies groups is unresolved.

IV. SUMMARY AND CONCLUSIONS

Since the early 1970s when it was first proposed, the reptation model has been the most popular and widely accepted description of dynamics in dense polymer systems.[1,4-8,37] Undoubtedly, it is a very elegant and simple model that can rationalize a number, but by no means all, of the experimental observations. Because of its relative maturity, it has been applied to a number of experimental situations. It is appropriate here to review its successes and failures. The model can reproduce the molecular weight dependence of the self-diffusion coefficient of linear chains, and it provides a scaling of the shear viscosity that goes like the cube of the molecular weight, whereas experiment indicates that it goes like the 3.4 power of the molecular weight. It predicts a $t^{1/4}$ regime in the mean square displacement profile of single beads, a regime seen in two simulations on linear chains. It predicts that the diffusion coefficient of a probe in a linear matrix should be independent of matrix molecular weight, that rings should move substantially slower than linear chains, and that stars should move exponentially slower in the number of arms than the corresponding linear chains. The reduction in mobility of stars predicted by

the reptation theory has been taken to vindicate the reptation/arm retraction mechanism.[90,91] However, the viscosity of rings[39,40] is in fact smaller than the corresponding linear chains, and granted that while the rings do not span as broad a molecular weight range as linear chains, they are in the 3.4 power of M regime for η, and it is difficult to understand why they are not moving slower if reptation, in fact, dominates.

In the present review we have summarized results from alternative theories that do not invoke the existence of a fixed tube, and yet the molecular weight dependence of D is recovered. In fact, the requirements for the $D \sim n^{-2}$ and the asymptotic matrix molecular weight independence of a probe diffusion constant follow from such weak considerations that no specific microscopic mechanism of D can be inferred from its molecular weight dependence.[16] Similarly, the existence of $t^{1/4}$ regimes in systems that cannot possibly reptate[17,65] shows once again that this too is a signature of cooperative dynamics and nothing more. With respect to different chain topologies, the analytic models are less developed, but just because a model isn't mature, it shouldn't be dismissed out of hand. A number of simulations on rings and linear chains do not find clear evidence for the existence of a fixed tube.[17,23,47,48,59,68,70,71] While there is some memory of the initial configuration (even free Rouse chains exhibit this at short enough times), as time increases for distances and times where the tube should be well-defined if reptation is correct (into the second $t^{1/2}$ regime of the single-bead autocorrelation function), the reptation component becomes of minor importance, and the environment surrounding the chains is not static; rather, cooperative back-flow effects are evident. This is true for both dynamic Monte Carlo[23,47,48,59,68,70,71] and Brownian dynamics simulations,[18] although this viewpoint has been questioned.[24,78]

These models, which treat the surroundings of a chain as a more fluid-like, and which view entanglements as being of a dynamic nature (although the exact mechanism is not understood), are equally successful as the reptation model in predicting the experimental phenomenology of linear chains. Moreover, these models agree with the simulation results. If one views the ability to treat the effects of different topology as the test of the validity of the theory, then reptation fails the test for ring melts. The development of alternative theories for ring and branched molecules is required before these theories can be dismissed or fully accepted. While the coupling model of Ngai[86] has been applied to stars, since it makes no attempt at specifying the precise microscopic mechanism of entanglements, it has been argued that it is not capable of verifying the dynamic entanglement picture. Undoubtedly this is true, but once again, if a general class of models fits the data, this implies that until such time as features peculiar to a particular motional mechanism are identified, then it is impossible to confirm the validity of a particular model.

In summary, while the problem of dynamics in dense polymer systems has

been the subject of study for the past 40 years, the precise mechanism of motion is not in fact resolved. A number of theories having quite a different physical basis can reproduce the experimental results, and because the simulation of a system well into the entangled regime is likely to remain beyond conputational capabilities for considerable time to come, the final disposition of the competing theories will not be fully resolved by recourse to simulation alone. (It can always be argued that if the desired reptation behavior is not seen, then the chains are too small.) As alternative analytic theories to reptation are more fully developed and applied to different chain topologies, and their predictions tested against experiment and simulation, then the controversy about whether reptation in a fixed tube is valid or not will hopefully be resolved. This review has attempted to make the case that the matter is not at all settled in favor of reptation in a fixed tube, and that an abundance of evidence exists that argues against the simple reptation model's validity. However, whether or not reptation ultimately proves valid, it was the first model that successfully rationalized a wide body of experimental data and provided a conceptual basis for the design of new experiments. In this alone, it has proven to be extremely valuable, and its importance to the field of polymer dynamics cannot be overemphasized.

Acknowledgment

The authors gratefully acknowledge the support of a grant from the polymer program of the National Science Foundation, No. DMR 85-20789. Useful discussions with Dr. K. Ngai, Dr. George Phillies and Dr. A. Sikorski are acknowledged.

References

1. W. W. Graessley, *Adv. Poly. Sci.* **46**, 67 (1982).
2. F. Bueche, *Physical Properties of Polymers*, Wiley, New York, 1962.
3. G. C. Berry and T. B. Fox, *Adv. Poly. Sci.* **5**, 261 (1968).
4. P. G. de Gennes, *J. Chem. Phys.* **55**, 572 (1971).
5. M. Doi and S. F. Edwards, *J. Chem. Soc.* **74**, 1789 (1978).
6. M. Doi and S. F. Edwards, *J. Chem. Soc.* **74**, 1802 (1978).
7. M. Doi and S. F. Edwards, *J. Chem. Soc.* **74**, 1818 (1978).
8. M. Doi and S. F. Edwards, *J. Chem. Soc.* **75**, 38 (1978).
9. H. Fujita and Y. Einaga, *Poly. J. (Tokyo)* **17**, 1131 (1985).
10. H. Fujita and Y. Einaga, *Poly. J. (Tokyo)* **17**, 1189 (1985).
11. G. Phillies, *Macromolecules* **20**, 558 (1987).
12. G. Phillies, *Macromolecules* **21**, 3101 (1987).
13. W. Hess, *Macromolecules* **19**, 1395 (1986).
14. R. W. Rendell, K. L. Ngai, and G. B. McKenna, *Macromolecules* **20**, 2250 (1987).
15. M. Fixman, *J. Chem. Phys.* **89**, 3892 (1988).
16. J. Skolnick, R. Yaris, and A. Kolinski, *J. Chem. Phys.* **86**, 1407 (1988).
17. J. Skolnick and R. Yaris, *J. Chem. Phys.* **86**, 1418 (1988).
18. M. Fixman, *J. Chem. Phys.* **89**, 3892 (1988).
19. M. Fixman, *J. Chem. Phys.* **89**, 3912 (1988).

20. A. Baumgartner, *Ann. Rev. Phys. Chem.* **35**, 419 (1984).
21. M. Bishop, D. Ceperley, H. L. Frisch, and M. M. Kalos, *J. Chem. Phys.* **76**, 1557 (1982).
22. M. T. Gurler, C. C. Crabb, D. M. Dahlin and J. Kovac, *Macromolecules* **36**, 398 (1983).
23. A. Kolinski, J. Skolnick, and R. Yaris, *J. Chem. Phys.* **86**, 1567 (1987).
24. K. Kremer, G. S. Grest, and I. Carmesin, *Phys. Rev. Lett.* **61**, 566 (1988).
25. W. W. Graessley, *Adv. Poly. Sci.* **16**, 1 (1974).
26. J. D. Ferry, *Viscoelastic Properties of Polymers*, Wiley, New York, 1980.
27. P. F. Green, P. J. Mills, C. J. Palmstrom, J. W. Mayer, and E. J. Kramer, *Phys. Rev. Lett.* **53**, 2145 (1984).
28. P. F. Green and E. J. Kramer, *Macromolecules* **19**, 1108 (1986).
29. M. Antonietti, J. Coutandin, R. Grutter, and H. Sillescu, *Macromolecules* **17**, 798 (1984).
30. M. Antonietti, J. Coutandin, and H. Sillescu, *Macromolecules* **19**, 793 (1986).
31 M. Tirrell, *Rubber Chem. Tech.* **57**, 523 (1984).
32. C. R. Bartels, B. Crist, and W. W. Graessley, *Macromolecules* **17**, 2702 (1984).
33. H. Yu in M. Nagasawa, *Molecular Conformation and Dynamics of Macromolecules in Condensed Systems* (*Studies in Polymer Science, Vol. 2*), Elsevier, Amsterdam, 1988, p. 107.
34. G. Phillies, *Macromolecules* **19**, 2367 (1986).
35. R. H. Colby, L. J. Fetters, and W. W. Graessley, *Macromolecules* **20**, 2226 (1987).
36. P. J. Flory, *Faraday Discuss. Chem Soc.* **68**, 14 (1979).
37. W. W. Graessley, *J. Poly Sci. Poly Phys. Ed.* **18**, 27 (1980).
38. J. Klein, *Macromolecules* **19**, 105 (1986).
39. G. B. McKenna, G. Hadziioannou, P. Lutz, G. Hild, C. Strazielle, C. Straupe, and A. J. Kovacs, *Macromolecules* **20**, 498 (1987).
40. J. Roovers, *Macromolecules* **21**, 1517 (1988).
41. P. Rouse, *J. Chem. Phys.* **21**, 1272 (1953).
42. H. Yamakawa, *Modern Theory of Polymer Solutions*, Harper and Row, New York, 1968.
43. K. E. Evans and S. F. Edwards, *J. Chem. Soc. Faraday Trans. 2* **77**, 1891 (1981).
44. K. E. Evans and S. F. Edwards, *J. Chem. Soc. Faraday Trans. 2* **77**, 1929 (1981).
45. S. F. Edwards and K. E. Evans, *J. Chem. Soc. Faraday Trans. 2* **77**, 1913 (1981).
46. P. G. de Gennes, *Scaling Concepts in Polymer Physics*, Cornell University Press, Ithaca, New York, 1979.
47. A. Kolinski, J. Skolnick, and R. Yaris, *J. Chem. Phys.* **86**, 7164 (1987).
48. A. Kolinski, J. Skolnick, and R. Yaris, *J. Chem. Phys.* **86**, 7174 (1987).
49. J. Skolnick, R. Yaris, and A. Kolinski, *Int. J. Mod. Phys. B.* **3**, 33 (1989).
50. A. Baumgartner and M. Muthukumar, *J. Chem. Phys.* **87**, 3082 (1987).
51. M. Muthukumar and A. Baumgartner, *Poly. Preprints* **30**, 99 (1989).
52. A. Baumgartner in *Applications of the Monte Carlo Method in Statistical Physics*, Springer-Verlag, Heidelberg, 1984.
53. K. Kremer, A. Baumgartner, and K. Binder, *J. Phys. A: Math Gen.* **15**, 2879 (1982).
54. H. J. Hilhorst and J. M. Deutch, *J. Chem. Phys.* **63**, 5153 (1975).
55. H. Boots and J. M. Deutch, *J. Chem. Phys.* **67**, 4608 (1977).
56. C. Stokely, C. C. Crabb, and J. Kovac, *Macromolecules* **19**, 860 (1986).
57. K. Binder in *Monte Carlo Methods in Statistical Physics*, Springer, Berlin, 1986.
58. P. H. Verdier and W. H. Stockmayer, *J. Chem. Phys.* **36**, 227 (1962).
59. J. Skolnick, A. Kolinski, A. Sikorski, and R. Yaris, *Poly. Preprints* **30**, 79 (1989).
60. M. Dial, K. S. Crabb, C. C. Crabb, and J. Kovac, *Macromolecules* **18**, 2215 (1985).
61. C. C. Crabb and J. Kovac, *Macromolecules* **18**, 1430 (1985).
62. K. Kremer, *Macromolecules* **16**, 1632 (1983).
63. A. Kolinski, J. Skolnick, and R. Yaris, *J. Chem. Phys.* **84**, 1922 (1986).
64. P. Romiszowski and W. H. Stockmayer, *J. Chem. Phys.* **80**, 485 (1984).

65. M. Milik, A. Kolinski, and J. Skolnick, *J. Chem. Phys.*, submitted.
66. S. F. Edwards, *Polymer* **6**, 143 (1977).
67. M. Antonietti, K. J. Folsch, and H. Sillescu, *Makromol. Chem.* **188**, 2317 (1987).
68. A. Sikorski, A. Kolinski, J. Skolnick, and R. Yaris, manuscript in preparation.
69. T. Pakula, *Macromolecules* **20**, 679 (1987).
70. T. Pakula and S. Geyler, *Macromolecules* **20**, 2909 (1987).
71. T. Pakula and S. Geyler, *Macromolecules* **21**, 1670 (1987).
72. M. E. Cates and J. M. Deutsch, *J. Phys.* **47**, 2121 (1986).
73. F. Bueche, *J. Chem. Phys.* **20**, 1959 (1952).
74. K. L. Ngai, R. W. Rendall, A. K. Rajagopal, and S. Teiter, *Ann. N.Y. Acad. Sci.* **484**, 150 (1985).
75. S. D. Levene and B. H. Zimm, *Science* **245**, 396 (1989).
76. L. S. Lehrman and H. Frisch, *Biopolymers* **21**, 995 (1982).
77. O. J. Lumpkin and B. H. Zimm, *Biopolymers* **21**, 2315 (1982).
78. K. Kremer, G. S. Grest, and B. Duenweg, *Poly. Preprints* **30**, 43 (1989).
79. E. Helfand, *Bell Syst. Tech J.* **58**, 2289 (1979).
80. Y. Einaga and H. Fujita, *Reorji Gakkaishi* **12**, 136 (1984).
81. W. Hess, *Macromolecules* **20**, 2587 (1987).
82. K. L. Ngai, A. K. Rajagopal, and S. Teitler, *J. Chem. Phys.* **88**, 5086 (1988).
83. C. A. Angel and M. Goldstein (Eds.), *Dynamic Aspects of Structural Change in Liquids and Glasses*, New York Academy of Sciences, New York, 1987, Vol. 284.
84. G. B. McKenna, K. L. Ngai, and D. J. Plazek, *Polymer* **26**, 1651 (1985).
85. K. L. Ngai, A. K. Rajagopal, and T. P. Lodge, *J. Poly. Sci., Poly. Phys. Ed.* submitted.
86. K. L. Ngai and T. P. Lodge, *J. Chem. Phys.* submitted.
87. R. S. Adler and K. Freed, *J. Chem. Phys.* **72**, 4186 (1980).
88. M. Daoud, J. P. Cotton, B. Farnoux, G. Jannink, G. Sarma, H. Benoit, R. Duplessix, C. Picot, and P. G. de Gennes, *Macromolecules* **8**, 805 (1975).
89. J. G. Kirkwood and J. Riseman, *J. Chem. Phys.* **16**, 565 (1948).
90. L. M. Wheeler and T. P. Lodge, *Macromolecules* **22**, 3399 (1989).
91. T. P. Lodge, P. Markland, and L. M. Wheeler, *Macromolecules* **22**, 3409 (1989).